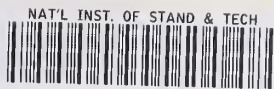


0875



A11106 200331

NIST  
PUBLICATIONS

NBSIR 73-280

# Thermodynamics of Chemical Species Important to Rocket Technology

Various authors

*filed under 1*

81184

*Chap. 1*

*- Coden -  
check ref.*

Physical Chemistry Division  
Institute for Materials Research  
National Bureau of Standards  
Washington, D. C. 20234

*Note:*

*Each Chap. is an  
abstract*

81185

*Chap. 2*

81186

*Chap. 3*

81187

*Chap. 4*

*do not want Chap 5+6*

1 January 1973

Final Report for Agreement No.  
AFOSR-ISSA-73-0001. Covering Period  
July - December 1972

Prepared for

QC

100

.456

no. 73-280

1973

C. 2

Office of Scientific Research  
Boulevard  
Virginia 22209



NBSIR 73-280

**THERMODYNAMICS OF CHEMICAL SPECIES  
IMPORTANT TO ROCKET TECHNOLOGY**

---

Various authors

Physical Chemistry Division  
Institute for Materials Research  
National Bureau of Standards  
Washington, D. C. 20234

1 January 1973

Final Report for Agreement No.  
AFOSR-ISSA-73-0001, Covering Period  
July - December 1972

Prepared for  
Air Force Office of Scientific Research  
1400 Wilson Boulevard  
Arlington, Virginia 22209



---

**U. S. DEPARTMENT OF COMMERCE, Frederick B. Dent, Secretary**  
**NATIONAL BUREAU OF STANDARDS, Richard W. Roberts, Director**



## FOREWORD

Structure, propulsion, and guidance of new or improved weapons delivery systems are dependent in crucial areas of design on the availability of accurate thermodynamic data. Data on high-temperature materials, new rocket propellant ingredients, and combustion products (including exhaust ions) are, in many cases, lacking or unreliable.

A broad integrated research program at the National Bureau of Standards supplies new or more reliable thermodynamic properties essential in several major phases of current propulsion development and application. Measured are compounds of those several chemical elements important in efficient propulsion fuels; those substances most affecting ion concentrations in such advanced propulsion concepts as ion propulsion; and the transition and other refractory metals (and their pertinent compounds) which may be suitable as construction materials for rocket motors, rocket nozzles, and nose cones that will be durable under extreme conditions of high temperature and corrosive environment. The properties determined extend in temperature up to 6000 degrees Kelvin. The principal research activities are experimental, and involve developing new measurement techniques and apparatus, as well as measuring heats of reaction, of fusion, and of vaporization; specific heats; equilibria involving gases; several properties from fast processes at very high temperatures; spectra of the infrared, matrix-isolation, microwave, and electronic types; and mass spectra. Some of these techniques, by relating thermodynamic properties to molecular or crystal structures, make it possible to tabulate reliably these properties over far wider ranges of temperature and pressure than those actually employed in the basic investigations. Additional research activities of the program involve the critical review of published chemical-thermodynamic (and some chemical-kinetic) data, and the generation of new thermochemical tables important in current chemical-laser research.

Previous reports describing related work have the NBS Report Nos.  
6297, 6484, 6645, 6928, 7093, 7192, 7437, 7587, 7796, 8033, 8186,  
8504, 8628, 8919, 9028, 9389, 9500, 9601, 9803, 9905, 10004, 10074,  
10326, 10481, and 10904.

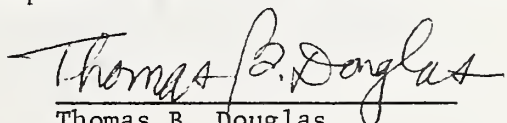
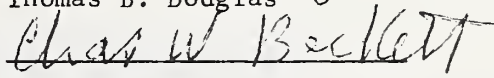
## ABSTRACT

This report (covering July-December 1972) and a subsequent report (covering January-June 1973) constitute the Final Reports on all past phases of the program except that measuring thermo-physical properties by high-speed techniques, which will be continuing. The nature and scope of the subjects covered in the present report may be inferred from the detailed Table of Contents to be found on the following pages.

The relative enthalpy of high-purity molybdenum was accurately measured over the temperature range 273-1173 K, and compared with all competing published data. Thermodynamic functions are given for 273-2100 K after smooth-joining with the best published data below 273 K and earlier NBS measurements 1170-2100 K. The heat capacity of a grade of graphite (AXM-5Q, Poco) was measured by a subsecond-duration pulse-heating technique 1500-3000 K. The results agreed to within 0.1% for two heating rates, and 0.6% for two different specimens, the estimated inaccuracy of the smoothed values being 3% or less.

Ideal-gas thermodynamic functions for  $\text{MoF}_5(\text{g})$  were computed and are tabulated for the temperature range 0-6000 K. These are based on earlier NBS infrared and Raman spectra of  $\text{MoF}_5$ , estimation of two unobservable fundamentals, and the assumption of  $D_{3h}$  symmetry with the Mo-F bond distance as in  $\text{MoF}_6$ . For deriving thermodynamic properties from combined transpiration and vapor-pressure data on a vapor such as  $\text{MoF}_5$  that may be highly associated, three alternative treatments are presented. One treatment is the classical-thermodynamic. The other two assume an infinite number of associated gas species, and numerical calculations illustrate the propagation of experimental errors.

The change in the normal spectral emittance (at 650 nm) of niobium during melting was measured using subsecond-duration resistive heating. Ten specimens deliberately varying in solid-state roughness from 0.1 to 0.95  $\mu\text{m}$  were used. Upon melting, the radiance temperature dropped by up to 35 K, and the emittance by up to 14% (the more so the greater the solid roughness). The radiance temperature of niobium was found to be 2425 K (IPTS-68) at the melting point, with an average absolute deviation of 0.6 K and a maximum deviation of 1.2 K using 12 specimens. This temperature was found to show no dependence on the initial surface conditions of the specimen.

  
Thomas B. Douglas  
  
Charles W. Beckett



# TABLE OF CONTENTS

	Page
Foreword . . . . .	i
Abstract . . . . .	iii
Chap. 1. <u>MOLYBDENUM: ENTHALPY MEASUREMENTS 273-1173 K, AND</u> <u>THERMODYNAMIC FUNCTIONS 273-2100 K</u> (by Thomas B. Douglas and David A. Ditmars) . . . . .	1
Abstract . . . . .	1
I. Introduction . . . . .	2
II. Sample . . . . .	3
Table 1. Mass spectrometric analysis of the molybdenum sample . . . . .	5
III. Calorimetric Procedure and Enthalpy Data . . . . .	6
Table 2. Enthalpy data for two empty 90 Pt-10 Rh containers. . . . .	8
Table 3. Enthalpy data for the molybdenum sample . . . . .	9
IV. Thermodynamic Functions, 273.15-2100 K . . . . .	10
Table 4. Thermodynamic functions for molybdenum (in terms of JOULES per mole) . . . . .	14
Table 5. Thermodynamic functions for molybdenum (in terms of CALORIES per mole) . . . . .	15
Fig. 1. Enthalpy compromise for the two sets of NBS measurements . . . . .	16
V. Comparison with Previous Investigators and Compilers . . . . .	17
Table 6. Outline of reported measurements of the enthalpy or heat capacity of molybdenum metal, 273-1200 K . . . . .	18
Table 7. Corrections for molybdenum, IPTS-48 to IPTS-68 . . . . .	20
Legend of Symbols for Figs. 2 & 3 . . . . .	21
Fig. 2. Comparison of $H^\circ - H^\circ_{273}$ , Mo, various investigators . . . . .	22
Fig. 3. Comparison of $C_p^\circ$ , Mo, various investigators . . . . .	23
Table 8. Comparisons of $H^\circ - H^\circ_{298.15}$ and $C_p^\circ$ for Mo in several critical compilations . . . . .	26
VI. References . . . . .	27
Chap. 2. <u>MEASUREMENT OF HEAT CAPACITY OF GRAPHITE IN THE</u> <u>RANGE 1500 TO 3000 K BY A PULSE HEATING METHOD</u> (by Ared Cezairliyan) . . . . .	31
Abstract . . . . .	31
Introduction . . . . .	32

## TABLE OF CONTENTS (Continued)

	<u>Page</u>
Method . . . . .	32
Measurements . . . . .	34
Experimental Results . . . . .	35
Table 1. Operational Characteristics of the Measurement System During the Experiments on Graphite-1 . . . . .	36
Table 2. Heat Capacity of Graphite (AXM-5Q, Poco) . . . . .	38
Fig. 1. Deviation of heat capacity results for graphite-1 from Equation (1) . . . . .	39
Estimate of Errors . . . . .	40
Fig. 2. Deviation of smoothed heat capacity results for graphite-1 and graphite-2 from Equation (1) . . . . .	41
Discussion . . . . .	43
Fig. 3. Heat capacity of various graphites reported in the literature . . . . .	44
Acknowledgement . . . . .	47
References . . . . .	48
 Chap. 3. <u>THERMODYNAMIC FUNCTIONS FOR MoF<sub>5</sub>(g)</u> (by Thomas B. Douglas, Ralph F. Krause, Jr., Nicolo Acquista, and Stanley Abramowitz) . . . . .	50
Molecular Constants Used for MoF <sub>5</sub> (g) . . . . .	51
References . . . . .	52
Table 1. Ideal-Gas Thermodynamic Functions for Molybdenum Pentafluoride Monomer (MoF <sub>5</sub> ) (in CALORIE energy units). . . . .	53
Table 2. Ideal-Gas Thermodynamic Functions for Molybdenum Pentafluoride Monomer (MoF <sub>5</sub> ) (in JOULE energy units) . . . . .	54
 Chap. 4. <u>ALTERNATIVE PROCEDURES IN INTERPRETING EQUILIBRIUM DATA ON PARTIALLY ASSOCIATED VAPORS</u> (by Thomas B. Douglas and Ralph F. Krause, Jr.) . . . . .	55
Abstract . . . . .	55
I. A Classical-Thermodynamic Interpretation . . . . .	56
II. Quasi-Chemical Interpretations . . . . .	59
III. Preliminary: A Combination of Data Yielding Ambiguous Thermodynamic Solutions . . . . .	59

# TABLE OF CONTENTS (Continued)

	<u>Page</u>
II2. Using Only Two Independent Data for Each Temperature . . . . .	62
II3. Using Three Independent Data for Each Temperature . . . . .	65
Table 1. An example illustrating errors in calculated values resulting from experimental errors in the input data . . .	70
III. References . . . . .	71
Chap. 5. <u>CHANGE IN NORMAL SPECTRAL EMITTANCE (AT 650 nm)</u> <u>OF NIOBIUM DURING MELTING AND ITS RELATION TO SURFACE</u> <u>ROUGHNESS</u> (by Ared Cezairliyan) . . . . .	73
Fig. 1. Variation of radiance temp- erature as a function of time for a niobium specimen near and at its melting point . . .	75
Fig. 2. Difference in normal spectral emittances of solid and liquid niobium at the melting point as a function of solid surface roughness . . . . .	76
Table 1. Summary of Experimental Results for Radiance Temp- erature and Normal Spectral Emittance (at 650 nm) of Niobium at its Melting Point .	77
References . . . . .	78
Chap. 6. <u>RADIANCE TEMPERATURE OF NIOBIUM AT ITS MELTING POINT</u> (by Ared Cezairliyan) . . . . .	79
Abstract . . . . .	79
1. Introduction . . . . .	80
2. General Considerations . . . . .	81
Fig. 1. Radiance temperature of pure metals near and at their melting points . . . . .	82
3. Method . . . . .	83
4. Measurements . . . . .	83
Fig. 2. Oscilloscope trace photograph of specimen radiance near and at its melting point as measured with the high-speed pyrometer .	85
5. Experimental Results . . . . .	86
Fig. 3. Variation of radiance temp- erature of niobium as a function of time near and at its melting point . . . . .	87

# TABLE OF CONTENTS (Continued)

	<u>Page</u>
Fig. 4. Radiance temperature at the peak and at the plateau for the niobium specimens . . . . .	88
Table 1. Summary of experiments for the measurement of radiance temperature of niobium during melting . . . . .	90
6. Estimate of Errors . . . . .	91
Fig. 5. Radiance temperature of niobium (with initially "smooth" surface) at its melting point . . . . .	92
Fig. 6. Radiance temperature of niobium (with initially "rough" surface) at its melting point . . . . .	93
Fig. 7. Differences of radiance temperature of niobium at its melting point for individual experiments . . . . .	95
7. Discussion . . . . .	96
8. References . . . . .	99

## Chapter 1

# MOLYBDENUM: ENTHALPY MEASUREMENTS 273-1173 K, AND THERMODYNAMIC FUNCTIONS 273-2100 K

by Thomas B. Douglas and David A. Ditmars

### Abstract

The enthalpy of a sample of molybdenum metal at least 99.8% pure was measured relative to 273 K at ten temperatures up to 1173 K, using accurate drop-calorimetric apparatus. In smoothing, the values were joined to recent enthalpy measurements on the metal by another NBS apparatus over the temperature range 1170-2100 K (enthalpy discrepancy at 1170 K, 0.3%) and to the results of published heat-capacity measurements below 273 K, to yield thermodynamic functions over the range 273-2100 K. The relative enthalpy and heat capacity over the range 273-1200 K are compared with the results of 17 previously published results of other investigators in the same temperature range.

## I. Introduction

The National Bureau of Standards has for many years sponsored the use of high-purity aluminum oxide as a high-temperature heat-capacity standard, and three years ago, on the basis of new NBS measurements using two different accurate apparatuses covering the respective temperature ranges 273.15-1173 K [29]<sup>1</sup> and 1173-2250 K, certified a standard sample of this material for this purpose over the combined temperature range [32]. As a check on accuracy, it is noteworthy that these two sets of results merged with but negligible discrepancy not only with each other but with earlier high-accuracy NBS adiabatic calorimetry on aluminum oxide both above and below 273 K.

Subsequently, molybdenum was proposed as an alternative heat-capacity standard that can be obtained in high purity, is like aluminum oxide free of transitions, has the advantages of a metallic material, and has an even higher melting point (about 2890 K). A special stock of this metal was procured, was characterized in great detail, and, by use of the same two apparatuses, measurement of its relative enthalpy has now been completed from 273 to 2100 K. However, issuance of the certified standard sample of molybdenum must await the completion of enthalpy measurements above 2100 K (perhaps to near the melting point using high-speed pulse calorimetry as well). This is prudent because the future data above

---

<sup>1</sup>Numbers in brackets refer to literature references at the end of this chapter.

2100 K can be expected to afford some refinement, however minor, of the thermodynamic properties well below 2100 K.

These NBS-sponsored results above 1170 K were reported two years ago [20], and those below 1170 K are being reported here for the first time, because the properties of molybdenum are of equal importance in Aerospace and other practical high-temperature applications. In fact, the AFOSR-sponsored research program at NBS has in recent years concentrated on the refractory transition metals, particularly on molybdenum metal, molybdenum-containing alloys, and molybdenum fluorides.

## II. Sample

The earlier NBS work on molybdenum (above 1170 K) failed to show any systematic difference in enthalpy between two samples of widely different types (one zone-refined, and about ten times as pure spectrochemically, but possibly less homogeneous, than the other). The present measurements were on only one specimen, that corresponding to Sample A of the earlier report [20]. That report may be consulted for details of the very extensive characterization of the sample. Important results are repeated below.

The sample from which the specimen for the present work (rods of 1/8" diameter) was taken had been previously drawn and annealed.

The results of spark-source mass spectrometry on a representative specimen are given in Table 1. (This analytical technique is in general agreement with the results of a qualitative spectrochemical analysis, summarized by footnotes to the table.) Note the near completeness of the coverage of chemical elements sought, and particularly the low levels of those low-atomic-weight elements analyzed for (to which the enthalpy and heat capacity of molybdenum, as calculated from the data, are particularly sensitive). Unfortunately, hydrogen was not analyzed for, and 0.01% by weight would be expected to make an error of the order of 1% if not corrected for; but it seems likely that the high-temperature history of the sample precluded the likelihood of more than a small fraction of this amount. According to Table 1, the total impurity adds to 0.02% by weight of the elements analyzed for, with the possibility of an upper limit of an additional 0.02% by weight of the elements (except F, Ne, and Ti) partially masked by major interference.

The result of an additional test, the measurement of the electrical-resistance ratio ( $R_{273.K}/R_{4.K}$ ) was interpreted as indicating a sample content of W, Ta, Nb, and Zr totaling 0.2 weight %. This far exceeds the levels of these elements shown in Table 1, but if true should contribute an error of the order of only 0.01% to the heat capacity, owing to the high atomic weights involved.

Table 1

Spark-source mass-spectrometric analysis for impurities in a representative specimen of the molybdenum sample, in ppm by weight<sup>a</sup>

Elements measured				Elements showing interference			
Element	ppm	Element	ppm	Element	ppm	Element	ppm
Ag <sup>d</sup>	1	Si <sup>c</sup>	40	Ar	< 20	N	< 10
Al <sup>b</sup>	7	V <sup>d</sup>	0.4	Au <sup>d</sup>	< 10	Nb <sup>d</sup>	< 3
As <sup>d</sup>	2	W <sup>d</sup>	56	Bd <sup>d</sup>	< 0.1	Ni <sup>d</sup>	< 20
Ca <sup>c</sup>	9	Zn <sup>d</sup>	0.26	Ba <sup>d</sup>	< 1	O	< 30
Cr <sup>d</sup>	12			C	< 3	Os <sup>d</sup>	< 6
Cu <sup>c</sup>	15			Cd <sup>d</sup>	< 8	Pd <sup>d</sup>	< 6
Fe <sup>b</sup>	40			Cl	< 0.1	Pt <sup>d</sup>	< 4
Ga <sup>d</sup>	0.1			Co <sup>d</sup>	< 7	Re	< 1
K	20			Cs	< 0.2	Rh <sup>d</sup>	< 0.2
Mn <sup>d</sup>	2			In <sup>d</sup>	< 0.5	S	< 1
Pd	0.6			Ir <sup>d</sup>	< 3	Sc <sup>d</sup>	< 0.3
Rb	0.3			Li	< 0.3	Sn <sup>d</sup>	< 30
Sb <sup>d</sup>	0.5			Mg <sup>c</sup>	< 31	Ta <sup>d</sup>	< 25

<sup>a</sup>In addition to the elements listed in the table, the following were reported as not detected and to be considered as present below stated amounts (all less than 1 ppm each; e.g., Be, < 0.01 ppm): Ac, Be, Bi, Br, Ce, Dy, Er, Eu, Ge, Gd, Hf, Hg, Ho, I, Kr, La, Lu, Nd, Pa, Pb, Pm, Po, Pr, Pu, Ra, Ru, Se, Sm, Sr, Tb, Tc, Te, Th, Tl, Tm, U, Xe, Y, Yb, and Zr. H and He were not analyzed for. Interference was complete for F, Ne, Na, and Ti; of these, Na was not detected by qualitative spectrochemical analysis, but the estimated detection limit in this case is 50 ppm.

<sup>b</sup>10-100 ppm each by qualitative spectrochemical analysis.

<sup>c</sup>< 10 ppm each by qualitative spectrochemical analysis.

<sup>d</sup>Not detected by qualitative spectrochemical analysis (generally, < 1 ppm).

### III. Calorimetric Procedure and Enthalpy Data

The relative enthalpy of the molybdenum was measured by drop calorimetry, which is described elsewhere in great detail [28]. The specific details of apparatus and procedure were identical in most respects with those described at length for the recent NBS measurements on aluminum oxide [29] mentioned in the Introduction (Section I). The molybdenum specimen had a mass of 20.8297 g (approximately 0.2 gram-atom), and was sealed in a 90 Pt-10 Rh container together with helium at several torr pressure. A Bunsen ice calorimeter measured the heat delivered by the specimen and its container in cooling from the temperature of the thermostated furnace to the ice-point (273.15 K). The presence of a long silver pipe around the sample (O.D. 2", I.D. 1"; and with silver "guard" rings at its end) greatly reduces temperature gradients in this apparatus, thus minimizing furnace-temperature error, which is undoubtedly the most common source of instrument error in most high-temperature drop calorimetry. The furnace temperature was measured up to 773 K by a platinum resistance thermometer, and above 773 K by two homogeneous Pt/90 Pt-10 Rh thermocouples; all three were calibrated at NBS on IPTS-48, but corrected [23] to the basis of the newer temperature scale (IPTS-68 [22]), on which all results in this chapter are based (since the new scale more nearly approximates the corresponding thermodynamic temperatures). Both thermocouples were compared up to 773 K with

the thermometer in place in the furnace, and a slight adjustment in their calibrations (0.1 K at and above 773 K) was made to avoid a temperature discontinuity at 773 K.

Since it was not practical to separately measure the enthalpy of the container actually used to hold the molybdenum, the required empty-container enthalpies were derived from enthalpy measurements on two entirely comparable containers in the aluminum-oxide work [29]. For completeness, these are listed in Table 2. (In any accurate drop calorimetry, including the present work, the empty container is measured separately in order that the reproducible but unknown heat lost during the drop cancel when the empty-container measured heat is subtracted from that for the container-plus-sample.) The smoothed empty-container "enthalpies" actually used are given by Eq (1) of Reference [29] (in J, at Kelvin temperature T, IPTS-68):

$$H_T - H_{273.15} = 4.529744(10^{-8})(T-273.15)^3 + 8.068654(10^{-5})(T-273.15)^2 + 1.901653(T-273.15) - 34.94647(T-273.15)/T \quad (1)$$

The individual measurements on the container-plus-sample, reduced to the basis of net relative enthalpy of the sample (see table footnote b) are listed in Table 3 in the order in which they were measured. (Actually, the measurements were made at temperatures slightly different from those in the first column, with corrections being made to the stated temperatures using published enthalpy data [25, 26]. Since these temperature deviations did not exceed 1 K, the uncertainties in these enthalpy corrections are far smaller than the precision of the data.)

Table 2

Enthalpy data for two empty 90 Pt-10 Rh containers

Temperature $T^a$	$H_T-H_{273.15}$ (measured)		Measured minus smoothed <sup>b</sup>	Temperature $T^a$	$H_T-H_{273.15}$ (measured)		Measured minus smoothed <sup>b</sup>
	Container 1	Container 2			Container 1	Container 2	
K	J	J	J	K	J	J	J
323.15 {	_____	90.67 90.21	+ 0.79 + 0.33	773.15 {	955.15 954.75	_____	+ 1.09 + 0.69
359.15 {	156.26 155.69	_____	+ 0.46 - 0.11	823.15 {	_____	1050.18 1052.21	- 4.32 - 2.29
423.15 {	_____	273.57 273.92	- 1.26 - 0.91	873.15 {	1156.64 1156.24	_____	+ 0.83 + 0.43
473.15 {	369.79 370.00	_____	+ 0.64 + 0.85	923.15 {	_____	1259.54 1260.75	+ 1.54 + 2.75
523.15 {	_____	464.00 464.57	- 0.46 + 0.11	973.15 {	1360.59 1360.38	_____	- 0.50 - 0.71
573.15 {	560.37 559.35	_____	- 0.32 - 1.34	1023.15 {	_____	1465.60 1464.14	+ 0.48 - 0.98
623.15 {	_____	659.13 657.64	+ 1.35 - 0.14	1073.15 {	1570.19 1569.03	_____	+ 0.09 - 1.07
673.15 {	756.37 756.97	_____	+ 0.67 + 1.27	1123.15 {	_____	1676.96 1676.14	+ 0.89 + 0.07
723.15 {	_____	854.99 854.56 853.88 854.21	+ 0.53 + 0.10 - 0.58 - 0.25	1173.15 {	1783.31 1782.61	_____	+ 0.25 - 0.45

<sup>a</sup>International Practical Temperature Scale of 1968 [22].<sup>b</sup>The "smoothed" values are those given by Eq. (1).

Table 3

Enthalpy data for the molybdenum sample

Temperature T <sup>a</sup> K	$H_T - H_{273.15}$ (measured), net for molybdenum sample <sup>b</sup> J mol <sup>-1</sup>	Measured minus smoothed	
		Based on Eq(3) <sup>c</sup> J mol <sup>-1</sup>	Based on Table 4 <sup>d</sup> J mol <sup>-1</sup>
323.15 {	1187.9	- 8.4	
	1196.2	- 0.1	
373.15 {	2410.6	- 11.5	
	2420.9	- 1.2	
473.15	4949.2	+ 5.9	
573.15	7540.2	+ 1.7	
673.15	10189.6	- 5.5	
773.15 {	12919.6	+ 14.0	
	12910.5	+ 4.9	
873.15	15662.2	- 3.2	
973.15	18470.6	- 0.7	
1073.15	21314.2	- 6.7	- 11.5
	24228.7	+ 15.9	- 11.2
1173.15 {	24206.9	- 5.9	- 33.0

<sup>a</sup>International Practical Temperature Scale of 1968 [22].

<sup>b</sup>Each value in this column was obtained from the corresponding gross measured heat by subtracting, from the gross, the smoothed value for the empty container (Eq (1)) and then scaling the remainder from the actual sample mass, 20.8297 g, to the "mole" (atomic) weight of molybdenum, 95.94 g [24].

<sup>c</sup>Eq (3) represents a "best fit" to the data in Column 2.

<sup>d</sup>Table 4 is based on Eq(3) below 1000 K, and on Eq(6) from 1000 to 1273.91 K.

The smoothing of the enthalpy data of Table 3, described in the next section, resulted in the deviations listed in the last two columns of the table.

#### IV. Thermodynamic Functions, 273.15-2100 K

The equations finally adopted to represent the thermodynamic functions of molybdenum, as based on the combined NBS work, are given later in this section as Eqs. (3)-(12), and were arrived at in the following manner.

Choosing trial fitting functions consistent with the known general shape of the  $C_p(T)$  curve of molybdenum and similar crystalline solids, the 14 values in the second column of Table 3 were used in the method of least squares to derive the coefficients of several alternative temperature functions, each required to vanish at  $T = 273.15$  and containing terms in  $T$ ,  $T^2$ , and one or more of  $\ln T$ ,  $T^{-1}$ , and  $T^{-2}$ . In addition, each such fitting was done giving equal weighting alternatively to each enthalpy measurement and to each temperature, since the better choice is debatable. Of the 14 fits tried, the "best" one had a standard deviation of residues of  $6.1 \text{ J mol}^{-1}$ . However, the next best fit ( $\sigma = 6.6 \text{ J mol}^{-1}$ ) was adopted because it proved to merge so well with the published data below 273.15 K as to require no adjustment. This equation is identical with Eq (3) (with proper choice of the constant term, and application of the equation over the whole temperature range 273-1173 K).

The "published data below 273.15 K" referred to in the preceding paragraph refers to an unpublished table of thermodynamic functions for molybdenum over the temperature range 0-360 K, prepared in 1968 by Reilly and Furukawa in an NSRDS program at the National Bureau of Standards [30]. This table was generated after critical examination of the published data then available, but follows closely the precise low-temperature heat capacities (10-273 K) of Clusius and Franzosini on 99.99% pure molybdenum [31]. The table, after adjustment from the IPTS-48 temperature scale to the basis of IPTS-68 [23], gives the same value of heat capacity as the derivative of Eq (3) at 278 K (but a 20% greater  $dC_p/dT$ ). The presently adopted equations for temperatures above 273.15 K [Eqs. (3)-(5)] assume the following values (identical to those of Reilly and Furukawa) at the ice-point:  $H_{273.15}^O - H_0^O = 3991 \text{ J mol}^{-1}$ , and  $S_{273.15}^O = 26.52 \text{ J mol}^{-1}\text{K}^{-1}$ .

The next step was to merge smoothly the equation representing the present measurements [Eq (3)] with that representing the earlier NBS measurements over 1170-2100 K, Eq (1) of Reference [20]. At the common temperature, 1173 K, the latter equation gives a value of  $H^O - H_{298}^O$  greater by  $78 \text{ J mol}^{-1}$  (which could be interpreted as equivalent to a temperature discrepancy of 2.6 K). The two equations were merged in the following manner: ( $T_0$ , A, and B being constants to be evaluated as below).

(a) Eqs. (3)-(5) were assumed to hold only up to 1000 K.

(b) For the temperature range 1000 K to  $T_0$ , the relative enthalpy was assumed to be represented by Eq (3) plus a term  $B(T-1000)^2 \text{ J mol}^{-1}$ .

(c) For the temperature range  $T_0$  to 2100 K, the relative enthalpy was assumed to be represented by Eq (1) of Reference [20] minus a term  $A(2100-T) \text{ J mol}^{-1}$ .

(d) The three constants  $T_0$ , B, and A were determined so as to give continuity in enthalpy and heat capacity, not only at 1000 K but also at  $T_0$ , and in addition to give a value of enthalpy at 1170 K half as far from the original "273-1173 K" equation (Eq. (3) of this work) as from the original "1170-2100 K" (Eq. (1) of Reference [20]) (in recognition of the greater temperature uncertainty in the latter work).

The above procedure led to the following values:

$$T_0 = 1273.91 \text{ K}; B = 0.000902 \text{ J mol}^{-1} \text{ K}^{-2}; A = 0.05005 \text{ J mol}^{-1} \text{ K}^{-1}. \quad (2)$$

With the additional requirement of continuity in the entropy at 1000 and 1273.91 K, the final equations for the relative enthalpy, heat capacity, and absolute entropy of molybdenum based on the NBS work then become [in terms of  $\text{J mol}^{-1}$  and T (K, IPTS-68), with "ln"  $\equiv$  natural logarithm]:

(A)  $T = 273.15$  to  $1000 \text{ K}$

$$H_T^0 - H_0^0 = 25.79244 T + 1.73410(10^{-3})T^2 - 862.870 \ln T + 1657.1 \quad (3)$$

$$C_p^0 = 25.79244 + 3.46820(10^{-3})T - 862.870/T \quad (4)$$

$$S^0 = 25.79244 \ln T + 3.46820(10^{-3})T + 862.870/T - 122.282 \quad (5)$$

(B) T = 1000 to 1273.91 K

$$H_T^O - H_0^O = 23.98844 T + 2.63610(10^{-3})T^2 - 862.870 \ln T + 2559.1 \quad (6)$$

$$C_P^O = 23.98844 + 5.27220(10^{-3})T - 862.870/T \quad (7)$$

$$S^O = 23.98844 \ln T + 5.27220(10^{-3})T + 862.870/T - 111.624 \quad (8)$$

(C) T = 1273.91 to 2100 K

$$H_T^O - H_0^O = 21.71415 T + 3.24129(10^{-3})T^2 + 1.590(10^6)\exp(-16000/T) - 1700.8 \quad (9)$$

$$C_P^O = 21.71415 + 6.48258(10^{-3})T + [2.544(10^{10})/T^2]\exp(-16000/T) \quad (10)$$

$$S^O = 21.71415 \ln T + 6.48258(10^{-3})T + 99.38[1 + (16000/T)]\exp(-16000/T) - 96.232 \quad (11)$$

Using Eqs. (3)-(11) and also the well-known thermodynamic equation for the Gibbs-energy function,

$$-(G^O - H_0^O) = S^O - [H^O - H_0^O]/T, \quad (12)$$

the thermodynamic functions were computed and are given in Table 4. Table 5 is a replica of Table 4 except in terms of the defined thermochemical calorie (= 4.1840 J).

The deviation plot of Fig. 1 shows the details of the compromise in the enthalpy merging above 1000 K described above. Although the heat-capacity function is continuous at all temperatures, its temperature derivative ( $dC_P/dT$ ) increases abruptly by 35% at 1000 K and again by 20% at 1273.91 K according to Eqs. (4), (7), and (10). It should, however, be pointed out that no evidence exists that these discontinuities in  $dC_P/dT$  arise from the sample itself.

Table 4

Thermodynamic functions for molybdenum (in terms of JOULES per mole)  
(International Practical Temperature Scale of 1968; 1 mole = 95.94 g)

T	$H^{\circ}-H_0^{\circ}$	$C_p^{\circ}$	$S^{\circ}$	$-(G^{\circ}-H_0^{\circ})/T$
K	J mol <sup>-1</sup>	J mol <sup>-1</sup> K <sup>-1</sup>	J mol <sup>-1</sup> K <sup>-1</sup>	J mol <sup>-1</sup> K <sup>-1</sup>
273.15	3991	23.58	26.52	11.91
275	4035	23.61	26.68	12.01
298.15	4585	23.93	28.60	13.22
300	4629	23.96	28.75	13.32
325	5232	24.26	30.68	14.58
350	5842	24.54	32.49	15.80
375	6459	24.79	34.19	16.97
400	7082	25.02	35.80	18.09
425	7710	25.24	37.32	19.18
450	8343	25.44	38.77	20.23
475	8982	25.62	40.15	21.24
500	9624	25.80	41.47	22.22
525	10272	25.97	42.73	23.17
550	10923	26.13	43.94	24.08
575	11578	26.29	45.11	24.97
600	12237	26.44	46.23	25.83
625	12900	26.58	47.31	26.67
650	13566	26.72	48.36	27.49
675	14236	26.86	49.37	28.28
700	14909	26.99	50.35	29.05
725	15585	27.12	51.30	29.80
750	16265	27.24	52.22	30.53
775	16947	27.37	53.11	31.25
800	17633	27.49	53.98	31.94
850	19013	27.73	55.66	33.29
900	20405	27.96	57.25	34.58
950	21809	28.18	58.77	35.81
1000	23223	28.40	60.22	36.99
1050	24651	28.70	61.61	38.13
1100	26093	29.00	62.95	39.23
1150	27551	29.30	64.25	40.29
1200	29023	29.60	65.50	41.32
1250	30511	29.89	66.72	42.31
1300	32013	30.21	67.89	43.27
1350	33532	30.57	69.04	44.20
1400	35069	30.93	70.16	45.11
1450	36625	31.31	71.25	45.99
1500	38200	31.70	72.32	46.85
1550	39796	32.11	73.37	47.69
1600	41412	32.54	74.39	48.51
1650	43050	32.98	75.40	49.31
1700	44711	33.45	76.39	50.09
1750	46396	33.95	77.37	50.86
1800	48106	34.47	78.33	51.61
1850	49843	35.01	79.28	52.34
1900	51607	35.58	80.22	53.06
1950	53401	36.18	81.16	53.77
2000	55226	36.81	82.08	54.47
2050	57083	37.47	83.00	55.15
2100	58974	38.16	83.91	55.83

Table 5

Thermodynamic functions for molybdenum (in terms of CALORIES per mole)  
(International Practical Temperature Scale of 1968; 1 cal = 4.1840 J; 1 mole = 95.94 g)

K	$\overset{\circ}{H}-\overset{\circ}{H}_0$ cal mol <sup>-1</sup>	$\overset{\circ}{C}_P$ cal mol <sup>-1</sup> K <sup>-1</sup>	$\overset{\circ}{S}$ cal mol <sup>-1</sup> K <sup>-1</sup>	$-(\overset{\circ}{G}-\overset{\circ}{H}_0)/T$ cal mol <sup>-1</sup> K <sup>-1</sup>
273.15	953.9	5.636	6.339	2.846
275	964.3	5.643	6.377	2.870
298.15	1095.8	5.720	6.836	3.160
300	1106.4	5.726	6.871	3.183
325	1250.5	5.799	7.332	3.485
350	1396.3	5.865	7.765	3.775
375	1543.7	5.925	8.171	4.055
400	1692.6	5.981	8.556	4.324
425	1842.7	6.032	8.920	4.584
450	1994.1	6.079	9.266	4.835
475	2146.7	6.124	9.596	5.077
500	2300.3	6.167	9.911	5.310
525	2455.0	6.207	10.213	5.537
550	2610.6	6.245	10.503	5.756
575	2767.2	6.283	10.781	5.968
600	2924.7	6.318	11.049	6.175
625	3083.1	6.353	11.308	6.375
650	3242.4	6.386	11.558	6.569
675	3402.4	6.419	11.799	6.759
700	3563.3	6.450	12.033	6.943
725	3724.9	6.481	12.260	7.122
750	3887.3	6.511	12.480	7.297
775	4050.5	6.541	12.694	7.468
800	4214.4	6.570	12.902	7.634
850	4544.3	6.626	13.302	7.956
900	4877.0	6.681	13.683	8.264
950	5212.4	6.735	14.045	8.559
1000	5550.5	6.787	14.392	8.842
1050	5891.7	6.860	14.725	9.114
1100	6236.5	6.932	15.046	9.376
1150	6584.8	7.003	15.356	9.630
1200	6936.8	7.074	15.655	9.875
1250	7292.2	7.143	15.945	10.112
1300	7651.2	7.220	16.227	10.342
1350	8014.3	7.305	16.501	10.565
1400	8381.7	7.393	16.768	10.782
1450	8753.6	7.483	17.029	10.992
1500	9130.1	7.577	17.285	11.198
1550	9511.4	7.675	17.535	11.398
1600	9897.6	7.777	17.780	11.594
1650	10289.1	7.884	18.021	11.785
1700	10686.1	7.996	18.258	11.972
1750	11088.8	8.114	18.491	12.155
1800	11497.5	8.237	18.722	12.334
1850	11912.6	8.368	18.949	12.510
1900	12334.4	8.504	19.174	12.682
1950	12763.2	8.648	19.397	12.852
2000	13199.3	8.798	19.618	13.018
2050	13643.2	8.956	19.837	13.182
2100	14095.1	9.120	20.055	13.343

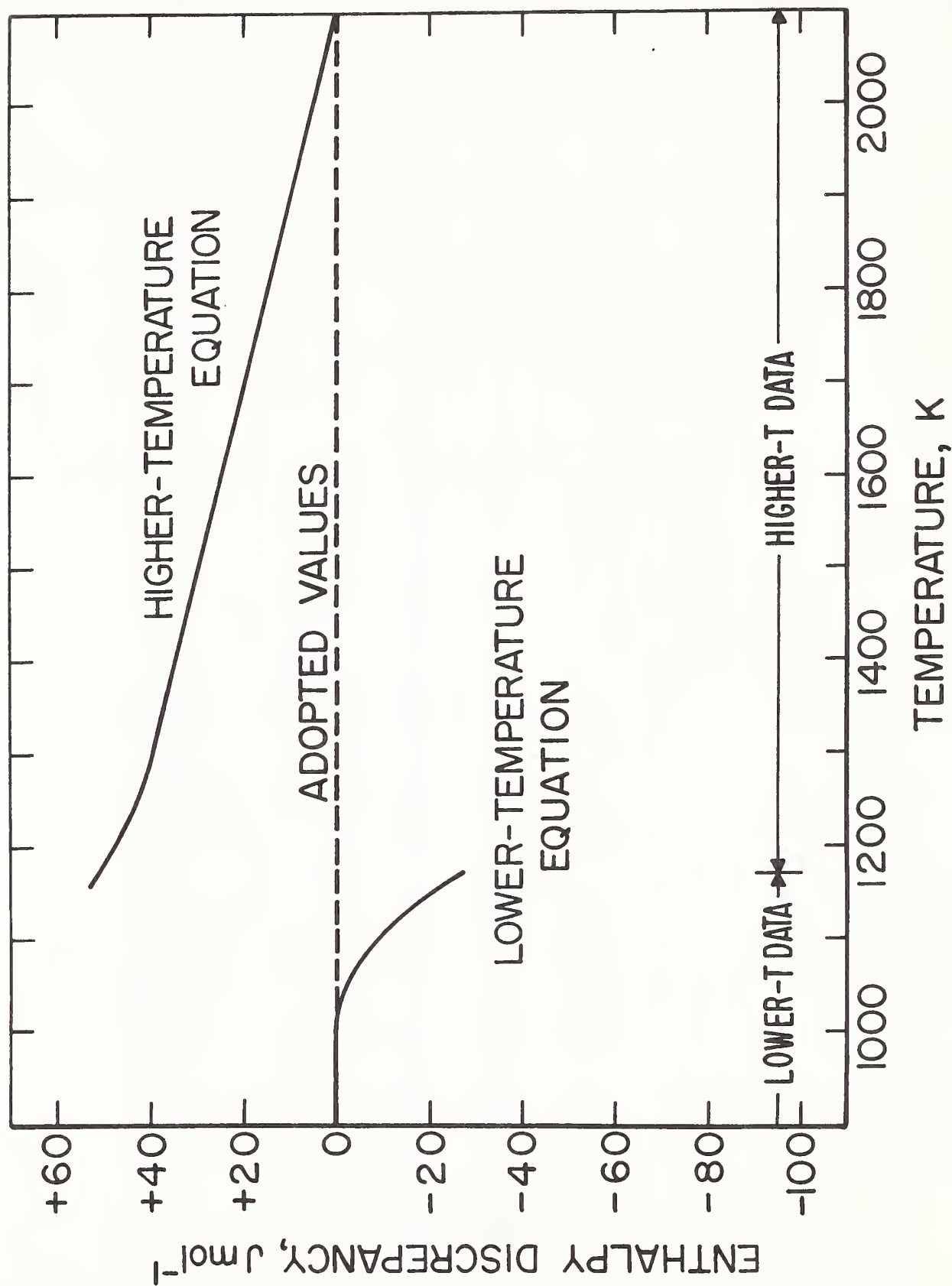


Fig. 1. Deviation plot showing the compromise made, for the relative enthalpy ( $H^\circ - H_{298}^\circ$ ) of molybdenum, between the two sets of NBS measurements. [The "lower-temperature equation" (Eq. (3)) represents the data below 1170 K; the "higher-temperature equation" (Eq. (1) of Ref. [20]) represents the data above 1170 K; and the "adopted values" correspond to Eqs. (3), (6), and (9) and Tables 4 and 5.]

Such "unreal" discontinuities in higher derivatives as formulated can sometimes be tolerated without doing serious injustice to the known facts. For example, there are marked discontinuities in the temperature derivative of the difference between temperatures on the IPTS-48 and IPTS-68 scales at 904 and 1338 K (Ref. [23], p. 466), and these discontinuities present small but real ambiguities in correcting heat capacities from one temperature scale to the other in the neighborhood of these two temperatures.

In view of the high purity of the molybdenum sample as described in Section II, it seems likely that the principal source of error in the smoothed values of the present work (273-1173 K) is inaccuracies in the measured temperatures of the sample in the furnace. It was estimated that the error in relative enthalpy  $H_T - H_{273}$  probably varies from 0.5% or less at  $T = 373$  to 0.1-0.2% at  $T = 1173$ , and that the error in heat capacity does not exceed 0.5% up to 1000 K.

#### V. Comparison with Previous Investigators and Compilers

The high practical importance of the high-temperature thermal properties of molybdenum metal is reflected in the large number of experimenters who have reported measurements of its enthalpy or heat capacity. Table 6 summarizes, in approximately chronological order, all these investigations found that report values in the temperature range of the present work (273-1173 K). These values (except a few which were not readily available) were first converted from the basis of IPTS-48 to IPTS-68 (unless the investigator

Table 6

Outline of reported measurements of the enthalpy or heat capacity of molybdenum metal in the temperature range 273-1200 K

Authors	Reference	Year	Method	Temp. Range (K) <sup>a</sup>	Remarks
Regnault	[1]	1840	Drop	273-373	2 determinations
Defacqz & Guichard	[2]	1901	Drop	288-717	Reported Mo 99.78% pure.
Stücker	[3]	1905	Drop	293-923	---
Wust et al.	[4]	1918	Drop	273-1773	---
Stern	[5]	1928	Drop	273-718	Documented temp. but not heat calibration.
Cooper & Langstroth	[6]	1929	Drop	233-563	Estimated Cp error: about 1%.
Bronson & Chisholm	[7]	1929	--	293-553	Mo stated 99.97% pure.
Bronson et al.	[8]	1933	Drop	254-774	---
Jaeger & Veenstra	[9]	1934	Drop	295-1828	Stated precision, 0.1-0.2%.
Redfield & Hill	[10]	1951	Drop	273-1359	Estimated enthalpy error: < 4%.
Lucks & Deem	[11]	1956	Drop	273-1882	Arc-melted Mo. measured $Al_2O_3$ also.
Fieldhouse et al.	[12]	1956	Drop	804-1898	---
Kothen	[13]	1957	Drop	298-1623	Only smoothed values reported.
Lehman	[14]	1960	Pulse heating	300-2800	Estimated Cp error, 1-2.5%.
Rasor & McClelland	[15]	1960	Pulse heating	1050-2890	Arc-melted Mo. 0.35% impurity. Estimated $\pm 5\%$ C error.
Taylor & Finch	[16]	1961	Pulse heating	200-2860	Estimated Cp error < 4% (< 2400 K).
Kirillin et al.	[17]	1961	Drop	299-2610	0.05% impurity (spectrochem.) Measured $Al_2O_3$ also.
Lazareva et al.	[18]	1961	Drop	1154-2462	0.02% impurity stated.
Pool et al.	[19]	1962	Drop	300-1300	---
Ishihara & Douglas	[20]	1971	Drop	1170-2102	Measurements on 3 high-purity samples.
Oetting & Navratil	[21]	1972	Drop	298-1381	0.02% impurity (spectrogr.).
Douglas & Ditmars	This report	1973	Drop	273-1173	Sample same as one of Ishihara & Douglas.

<sup>a</sup>In using the drop method the calorimeters were almost invariably near room temperature, so the listing of a much higher "lower" temperature indicates the lack of enthalpy data at intervening temperatures.

defined his temperature scale in terms of recognized fixed points). (See Table 7 for the magnitudes of these corrections.) The values were then compared with those from the measurements reported here. (For a similar comparison with the NBS work in the temperature range 1170-2100 K, see Ref. [20].) The comparisons are shown graphically in Figs. 2 and 3.

Figure 2 is a deviation plot of the enthalpy relative to 273.15 K. The base line represents Eqs. (3) and (6) (or Table 4 or 5), and the points represent the percentage deviations, from this base, of unsmoothed values (including those of Table 3), corrected to a base temperature of 273.15 K when necessary, using Eq (3). (Curves are given in those cases where only smoothed values were reported, but no attempt was made to include in Fig. 2 the corresponding enthalpies of those investigators who measured and reported only heat capacities.) In many cases "repeat" individual measurements were reported over the same or nearly the same temperature range, and in such cases only the average is plotted, to simplify the graph.

Figure 3 shows total heat capacity vs. temperature. The solid curve corresponds to Eqs. (4) and (7) (or Table 4). The individual points are unsmoothed values, and some of them are from investigators who measured heat capacity but not enthalpy. Other points correspond to heat-capacity values calculated from unsmoothed

Table 7

Corrections for molybdenum to convert from the basis of  
 IPTS-48 to the basis of IPTS-68 (see ref. [23])

Temperature T	$(H_T - H_{273})_{68} - (H_T - H_{273})_{48}$	$(C_P)_{68} - (C_P)_{48}$
K	J mol <sup>-1</sup>	J mol <sup>-1</sup> K <sup>-1</sup>
300	+ 0.2	+ 0.004
400	- 0.3	- 0.011
500	- 1.3	- 0.010
600	- 2.1	- 0.003
700	- 2.2	0.000
800	- 2.5	- 0.011
900	- 5.3	- 0.054
1000	- 13.1	- 0.082
1100	- 21.5	- 0.086
1200	- 30.5	- 0.092
1300	- 39.8	- 0.098
1400	- 47.3	- 0.062
1500	- 53.7	- 0.069
1600	- 60.8	- 0.076
1700	- 68.6	- 0.085
1800	- 77.3	- 0.095
1900	- 86.8	- 0.106
2000	- 97.3	- 0.119
2100	- 109.0	- 0.134

# LEGEND OF SYMBOLS FOR FIGURES 2 AND 3

	NBS work (smoothed) [Eqs (3)-(11) and Tables 4 & 5]
	Kothen, 1957 (smoothed) [13]
	Bronson & Chisholm, 1929 (smoothed) [7]
	Taylor & Finch, 1961 (smoothed) [16]
	Douglas and Ditmars, 1973 [this report]
	Bronson, Chisholm, & Dockerty, 1933 [8]
	Lazareva <u>et al.</u> , 1961 [18]
	Cooper & Langstroth, 1929 [6]
	Wust <u>et al.</u> , 1918 [4]
	Jaeger & Veenstra, 1934 [9]
	Stucker, 1905 [3]
	Defacqz & Guichard, 1901 [2]
	Ishihara & Douglas, 1971 [20]
	Regnault, 1840 [1]
	Redfield and Hill, 1951 [10]
	Lehman, 1960 [14]
	Lucks & Deem, 1956 [11]
	Stern, 1928 [5]
	Oetting & Navratil, 1972 [21]
	Kirillin <u>et al.</u> , 1961 [17]

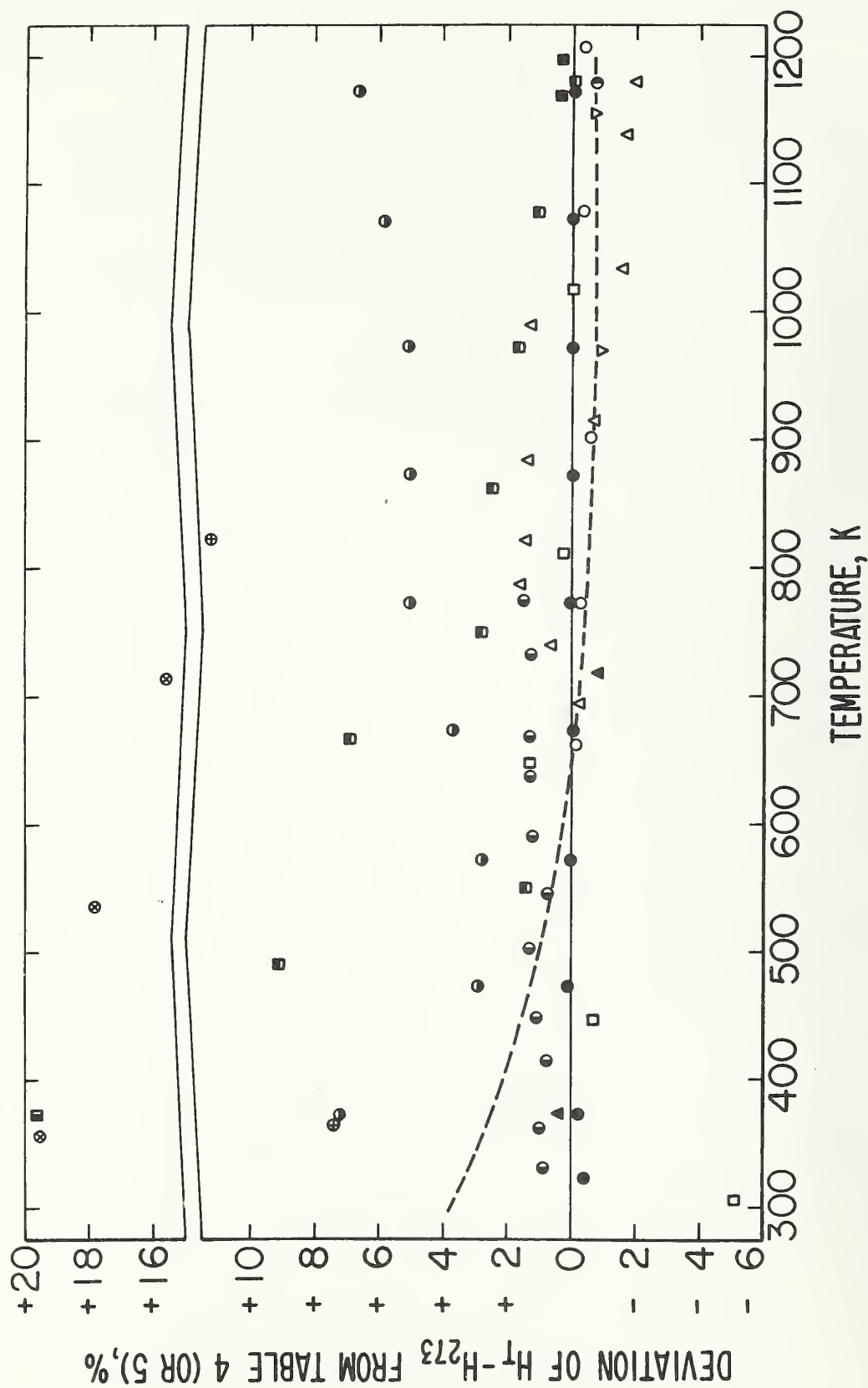


Fig. 2. Comparison of molybdenum  $H-H_{273}^O$  values of various investigators. [See neighboring page for legend of symbols.]

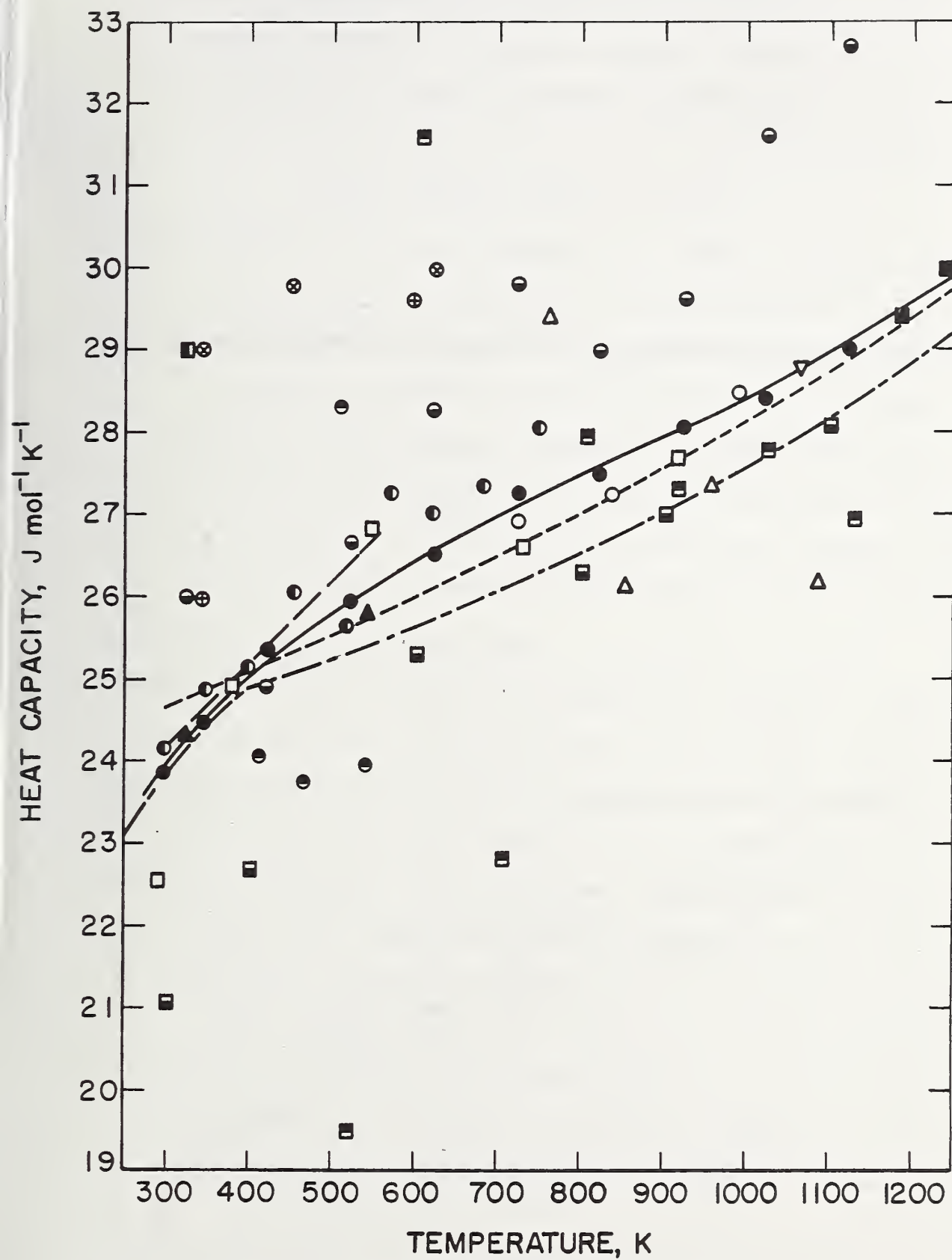


Fig. 3. - Comparison of molybdenum heat-capacity values of various investigators. [See neighboring page for legend of symbols.]

enthalpies at successive temperatures:  $\Delta H/\Delta T$  except when  $\Delta T$  was several hundred degrees. In this case the small curvature corrections were applied (when appreciable) from the approximate equation

$$C_p(\text{at } T_m) = \Delta H/\Delta T - (1/24)(d^2C_p/dT^2), \quad (13)$$

where  $T_m$  is the middle of the temperature interval, and where  $d^2C_p/dT^2$

was calculated from Eq. (4) or (7). In plotting  $C_p$  values thus derived from enthalpy data, an attempt was made to group an observer's points and average them such that the intervals  $\Delta T$  were approximately 50 to 100 degs (as in the present measurements). This leads to a fairer comparison of precision from one investigator to another, since even good enthalpy precision would lead to an enormous scatter of  $\Delta H/\Delta T$  values if  $\Delta T$  were sufficiently small.

Figures 2 and 3 show that, aside from the earliest measurements, most of the earlier investigators agree in this temperature range with the present work to within 2 to 3% on relative enthalpy, and to within 5% on heat capacity. For high temperatures the accuracy of temperature measurement is always suspected as a major source of error. But for lower temperatures (particularly those determined by the ice and steam points), large deviations in the values cast serious doubt on the calorimetry, and this is notably true of the earliest measurements. Also to be questioned is the purity of some of the molybdenum samples used, particularly since small percentages of unsuspected impurities of low atomic weight often lead to enthalpies and heat capacities that are too high

by several times the impurity percentage. In this connection it might be mentioned that, in contrast to the very thorough analysis of the NBS sample (Table 1) and the less comprehensive analyses reported for many of the others, several investigators merely reported that their samples were gifts and that they "ought to be pure."

The deviations from the adopted results of this report [Eqs (3)-(11), or Table 4 or 5] are listed in Table 8 for three well-known critical compilations. These deviations reflect some of the general trends noticeable in Figures 2 and 3, since the compiled values necessarily depend on the literature available up to several years ago.

Table 8

Absolute deviations of relative enthalpy and percentage deviations of heat capacity from Table 4 (or 5), as adopted in several current critical compilations

Temperature T K	Deviation of $H_T - H_{298.15}$			Deviation of $C_p$		
	Kelley[25] J mol <sup>-1</sup>	Hultgren et al.[26] J mol <sup>-1</sup>	JANAF[27] J mol <sup>-1</sup>	Kelley[25] %	Hultgren et al.[26] %	JANAF[27] %
300	0	0	+ 2	- 0.8	+ 0.5	+ 0.2
400	- 8	+ 5	+ 18	- 2.4	- 0.1	+ 1.1
500	0	0	+ 51	- 2.6	- 0.3	+ 1.2
600	- 19	- 6	+ 78	- 2.3	- 0.3	+ 1.0
700	- 35	- 25	+ 96	- 1.7	- 0.9	+ 0.4
800	- 81	- 63	+ 100	- 1.0	- 1.3	- 0.3
900	- 138	- 111	+ 77	- 0.3	- 1.7	- 1.1
1000	- 210	- 158	+ 30	+ 0.5	- 1.1	- 1.6
1100	- 236	- 183	- 20	+ 0.7	- 0.8	- 1.3
1200	- 246	- 193	- 89	+ 1.1	- 0.2	- 2.4
1300	- 233	- 196	- 154	+ 1.3	+ 0.2	- 2.1
1400	- 201	- 185	- 215	+ 1.3	+ 0.4	- 1.8
1500	- 201	- 172	- 269	+ 1.0	+ 0.4	- 1.6
1600	- 156	- 165	- 315	+ 0.5	+ 0.1	- 1.4
1700	- 157	- 170	- 362	- 0.2	- 0.4	- 1.4
1800	- 173	- 197	- 407	- 1.1	- 1.2	- 1.5
1900	- 254	- 257	- 466	- 2.3	- 2.2	- 1.8
2000	- 369	- 359	- 535	- 3.7	- 3.5	- 2.2
2100	- 530	- 516	- 629	- 5.3	- 4.9	- 2.8

## VI. References

- [1] M. V. Regnault, Ann. chim. phys. [2] 73, 5 (1840).
- [2] E. Defacqz and M. Guichard, Ann. chim. phys. [7] 24, 139-144 (1901).
- [3] N. Stücker, Sitzb. konig. Akad. Wiss., Wien, 114, 657 (1905).
- [4] F. Wüst, A. Meuthen, and R. Durrer, Forsch. Arb. Ver. deut. Ing., No. 204 (1918).
- [5] T. E. Stern, Phys. Rev. [2] 32, 298-301 (1928).
- [6] D. Cooper and G. O. Langstroth, Phys. Rev. 33, 243-248 (1929).
- [7] H. L. Bronson and H. M. Chisholm, Proc. Nova Scotia Inst. Sci. 17, 44-45 (1929) (cf. Chem. Abstr. 26, 4532-4533 (1932)).
- [8] H. L. Bronson, H. M. Chisholm, and S. M. Dockerty, Can. J. Research 8, 282-303 (1933).
- [9] F. M. Jaeger and W. A. Veenstra: (a) Proc. Royal Acad. Amsterdam 37, 61-66 (1934) (in Eng.); (b) Rec. Trav. Chim. Pays-Bas 53, 677-687 (1934) (in Eng.).
- [10] T. A. Redfield and J. H. Hill, Report ORNL-1087, Oak Ridge National Laboratory, Oak Ridge, Tenn. (1951).
- [11] C. F. Lucks and H. W. Deem, WADC Tech. Report 55-496 (ASTIA Document AD 97185) (1956).

- [12] I. B. Fieldhouse, J. C. Hedge, J. I. Lang, A. N. Takata, and T. E. Waterman, WADC Tech. Report 55-495 (1956).
- [13] C. W. Kothen, Diss. Abstr. 17, 2842-2844 (1957).
- [14] G. W. Lehman, WADD Tech. Report 60-581 (1960).
- [15] N. S. Rasor and J. D. McClelland, J. Phys. Chem. Solids 15, 17-26 (1960).
- [16] R. E. Taylor and R. A. Finch, J. Less Common Metals 6, 283-294 (1963) [cf. Report NAA-SR-6034 (Metals, Ceramics, and Materials), Atomics International, Canoga Park, Calif. (1961)].
- [17] N. A. Kirillin, A. E. Sheindlin, and V. Y. Chekhovskoi: (a) Dokl. Akad. Nauk SSSR 139, 645-647 (1961); (b) Int. J. Heat Mass Transfer 5, 1-9 (1962) (in Eng.).
- [18] L. S. Lazareva, P. B. Kantor, and V. V. Kandyba, Fiz. Met. i. Metallov 11, 628-629 (1961) (English: Phys. Metals and Metallog. 11, 133-134 (1961)).
- [19] M. J. Pool, R. W. Sullivan, and C. E. Lundlin, Quarterly Status Rept. No. 9, contract AF 19(604)-7222, U. of Denver, Denver Research Inst., Denver, Colo. (1962).
- [20] S. Ishihara and T. B. Douglas, NBS Report 10481 (AFOSR-TR-71-2584), National Bureau of Standards, Washington, D. C. (1971), pp. 59-83.

- [21] F. L. Oetting and J. D. Navratil, J. Chem. Eng. Data 17, 230-231 (1972).
- [22] "The International Practical Temperature Scale of 1968", Metrologia 5, 35 (1969).
- [23] T. B. Douglas, J. Research Nat. Bur. Stand. (U. S.) 73A, 451-470 (1969).
- [24] A. E. Cameron and E. Wichers, J. Am. Chem. Soc. 84, 4175 (1962).
- [25] K. K. Kelley, U. S. Bur. Mines Bull. 584, p. 125 (1960) (manuscript completed Nov. 1958).
- [26] R. Hultgren, R. L. Orr, P. D. Anderson, and K. K. Kelley, "Selected Values of Thermodynamic Properties of Metals and Alloys," Univ. of Calif., Berkeley, Calif. (table for Mo: March 1965).
- [27] JANAF Thermochemical Tables, 2nd ed., Nat. Stand. Ref. Data Series, Nat. Bur. Stand. (U. S.), 37, 1141 pages (1971) (table for Mo(c): Dec. 1966).
- [28] T. B. Douglas and E. G. King, "High Temperature Drop Calorimetry," Chapter 8 in "Experimental Thermodynamics," Vol. I (Butterworths, London, 1968); also in "Precision Measurement and Calibration (Heat)", D. C. Ginnings, Ed., Nat. Bur. Stand. (U. S.), Spec. Publ. 300, Vol. 6, 181-219 (1970).

- [29] D. A. Ditmars and T. B. Douglas, J. Research Nat. Bur. Stand. (U. S.) 75A, 401-420 (1971).
- [30] M. L. Reilly and G. T. Furukawa, National Bureau of Standards, Washington, D. C., private communication.
- [31] K. Clusius and P. Franzosini, Zeit. Naturforsch. 14a, 99-105 (1959).
- [32] Certificate: "Standard Reference Material 720, Synthetic Sapphire ( $Al_2O_3$ )," National Bureau of Standards, Washington, D. C., 1970.

Chapter 2

MEASUREMENT OF HEAT CAPACITY OF  
GRAPHITE IN THE RANGE 1500 TO 3000 K

BY A PULSE HEATING METHOD<sup>1</sup>

Ared Cezairliyan

National Bureau of Standards

Washington, D. C. 20234

ABSTRACT

Measurement of heat capacity of a grade of graphite (AXM-5Q, Poco) in the temperature range from 1500 to 3000 K by a subsecond duration pulse heating technique is described. The results for the same specimen corresponding to two different heating rates are in agreement within 0.1%. The results for two different specimens are in agreement within 0.6%. The heat capacity of graphite in the temperature range from 1500 to 3000 K is expressed by the following function (standard deviation = 0.5%):

$$c_p = 19.12 + 4.236 \times 10^{-3} T - 5.919 \times 10^{-7} T^2$$

where  $T$  is in K, and  $c_p$  is in  $\text{J mol}^{-1} \text{K}^{-1}$ . The inaccuracy of reported results is estimated to be not more than 3%.

---

<sup>1</sup>This work was supported in part by the U. S. Air Force Office of Scientific Research.

## INTRODUCTION

Considerable disagreements exist between the limited number of experimental results for the heat capacity of graphite reported in the literature above 1500 K. Most of the reported measurements were performed on different grades of graphite, which complicate their evaluation and pose the question whether the differences were due to measurement errors or were indicative of the differences in the graphite grades.

As an attempt to elucidate this, a program was initiated for the systematic and accurate measurement of heat capacity of various grades of graphite at high temperatures. The objective of this paper is to present the results of the first phase, namely the measurement of heat capacity of a grade of graphite (AXM-5Q, Poco) in the temperature range from 1500 to 3000 K. The measurements were performed utilizing a subsecond duration pulse heating technique.

## METHOD

The method is based on rapid resistive self-heating of the specimen from room temperature to high temperatures (above 1500 K) in less than one second by the passage of electrical currents through it; and on measuring, with millisecond resolution, experimental quantities such as current through the specimen, potential drop across the specimen, and specimen temperature.

Current through the specimen is determined from the measurement of the potential difference across the standard resistance placed in series with the specimen. Potential difference across the middle one third of the specimen is measured using spring-loaded, knife-edge probes. Specimen temperature is measured at the rate of 1200 times per second with a high-speed photoelectric pyrometer [1]<sup>2</sup>. A small hole in the wall at the middle of the tubular specimen provides an approximation to blackbody conditions. The experimental quantities are recorded with a digital data acquisition system, which has a time resolution of 0.4 millisecond and a full-scale signal resolution of one part in 8000.

Details regarding the construction and operation of the measurement system, the methods of measuring experimental quantities, and other pertinent information, such as formulation of relations for properties, etc. are given in earlier publications [2, 3].

---

<sup>2</sup>Figures in brackets indicate the literature references at the end of this paper.

## MEASUREMENTS

The measurements were performed on two tubular specimens, designated as graphite-1 and graphite-2, which were fabricated from the same graphite block<sup>3</sup>. The nominal dimensions of the specimens were: length, 76 mm; outside diameter, 6.3 mm; and wall thickness, 0.5 mm. The specimens were 99.99<sup>+</sup> pure. Before the start of the experiments, the specimens were annealed by subjecting them to 20 heating pulses (up to 2800 K). The experiments were conducted with the specimens in a vacuum environment of approximately  $10^{-5}$  torr.

To study possible effects that may be attributable to the rate with which the specimen heats, two different heating rates, designated as "fast" and "slow", were used in the experiments on graphite-1. To optimize the operation of the high-speed pyrometer, the temperature interval (1500 to 3000 K) was divided into six ranges. One experiment was performed in each range for each heating rate. This yielded a total of 12 experiments for graphite-1. In the case of graphite-2, only the "fast" heating rate was used and 4 experiments were performed to cover the range 1500 to 2200 K.

---

<sup>3</sup>The graphite block (AXM-5Q, Poco) was furnished by the U. S. Air Force Materials Laboratory, Wright-Patterson Air Force Base, Ohio.

To optimize the operation of the measurement system, the heating rate of the specimen (in both "fast" and "slow" cases) was varied depending on the desired temperature range by adjusting the value of the resistance in series with the specimen. The operational characteristics of the measurement system, during the present experiments such as current pulse length, specimen heating rate, and heat loss from the specimen by thermal radiation, are summarized in Table 1.

Optical checks performed on the experiment chamber window after the pulse experiments did not indicate any graphite deposition. Also, weight measurements before and after the entire set of pulse experiments did not show any change in the specimen weight. However, trial experiments above 3000 K, indicated graphite evaporation both in vacuum and in argon environment at atmospheric pressure. For this reason, with the present system it was not possible to extend the accurate measurements above 3000 K.

#### EXPERIMENTAL RESULTS

Heat capacity was determined from the experimental data on current, voltage, and temperature obtained during the rapid heating period. A correction for heat loss due to thermal radiation was made based on data obtained during the initial radiative cooling period following the heating period. The procedure for determining properties from experimental data is given in an earlier publication [3].

Table 1

## Operational Characteristics of the Measurement System

## During the Experiments on Graphite-1

Quantity	Heating Rate		Temp. K
	"Fast"	"Slow"	
Current pulse length (ms)	210	280	1500
	280	510	3000
Specimen heating rate (K s <sup>-1</sup> )	6000	4400	1500
	6200	2700	3000
Radiative heat loss from specimen (% of input power)	2	3	1500
	7	10	2000
	13	22	2500
	26	45	3000

The heat capacity results obtained for the "fast" and "slow" experiments were fitted separately to quadratic functions in temperature using the least squares method. Standard deviation of an individual point from the smooth function is 0.5% and 0.4% for the "fast" and "slow" experiments, respectively. The average absolute difference between the heat capacity results of the "fast" and "slow" experiments for graphite-1 over the range 1500 to 3000 K is 0.1% with a maximum difference of 0.2%. Since this difference is within the imprecision of the measurements, the final results for graphite are obtained by combining the experimental results corresponding to both heating rates for graphite-1. The function for heat capacity (standard deviation = 0.5%) that represents the results in the temperature range 1500 to 3000 K is:

$$c_p = 19.12 + 4.236 \times 10^{-3}T - 5.919 \times 10^{-7}T^2 \quad (1)$$

where  $T$  is in K, and  $c_p$  is in  $\text{J mol}^{-1}\text{K}^{-1}$ . Heat capacity of graphite computed using Equation (1) is given in Table 2. All the results reported in this paper are based on the International Practical Temperature Scale of 1968 [4].

Figure 1 shows the deviation of the experimental results of graphite-1 corresponding to "fast" and "slow" heating rates from the smooth function represented by Equation (1).

Table 2

Heat Capacity of Graphite (AXM-5Q, Poco)

T (K)	$c_p$ (J mol <sup>-1</sup> K <sup>-1</sup> )
1500	24.14
1600	24.38
1700	24.61
1800	24.83
1900	25.03
2000	25.22
2100	25.41
2200	25.57
2300	25.73
2400	25.88
2500	26.01
2600	26.13
2700	26.24
2800	26.34
2900	26.43
3000	26.50

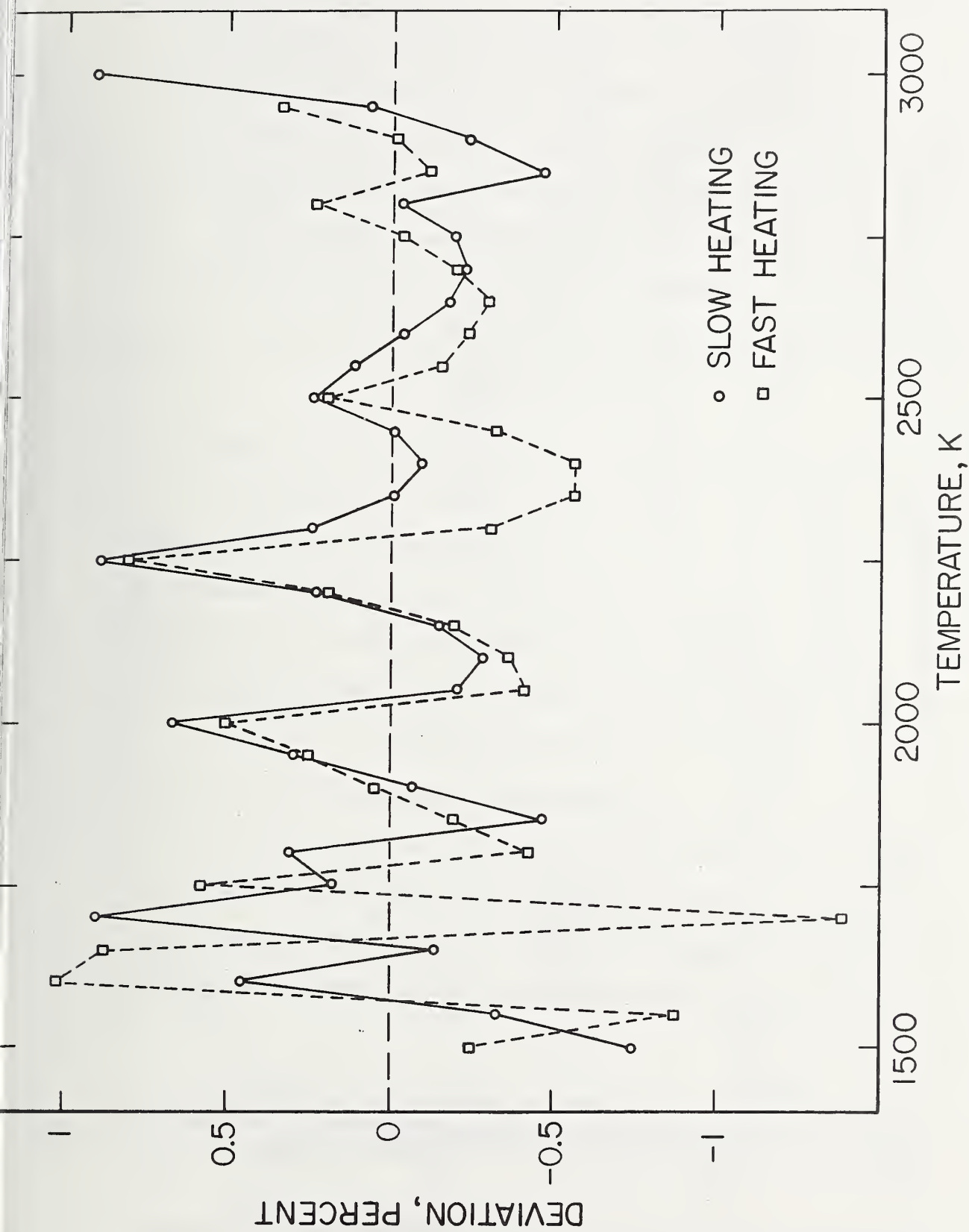


Figure 1. Deviation of heat capacity results for graphite-1 from Equation (1).

The deviation of the smooth functions for the "fast" and "slow" experiments for graphite-1 from the final combined function, Equation (1), is presented in Figure 2. In the same figure, the deviation of the results for graphite-2 from those of graphite-1 is also shown. The average absolute difference between the heat capacity results of graphite-2 and those of graphite-1 (combined) is 0.6%, with a maximum difference of 0.7%.

#### ESTIMATE OF ERRORS

The details for estimating errors in measured and computed quantities in high-speed experiments using the present measurement system are given in an earlier publication [3]. In this paper, the specific items in the error analysis were recomputed whenever the present conditions differed from those in the earlier publication. The imprecision<sup>4</sup> in the measurements is 0.5%. The inaccuracy<sup>5</sup> in the results is estimated to be not more than 3%.

Because of the high value of hemispherical total emittance of graphite, heat loss from the specimen due to thermal radiation constitutes a substantial fraction of the input power, especially at temperatures above 2500 K (Table 1). In the present work, the uncertainty in measuring heat loss by thermal radiation is estimated

---

<sup>4</sup>Imprecision refers to the standard deviation of an individual point as computed from the difference between measured value and that from the smooth function obtained by the least squares method.

<sup>5</sup>Inaccuracy refers to the estimated total error (random and systematic).

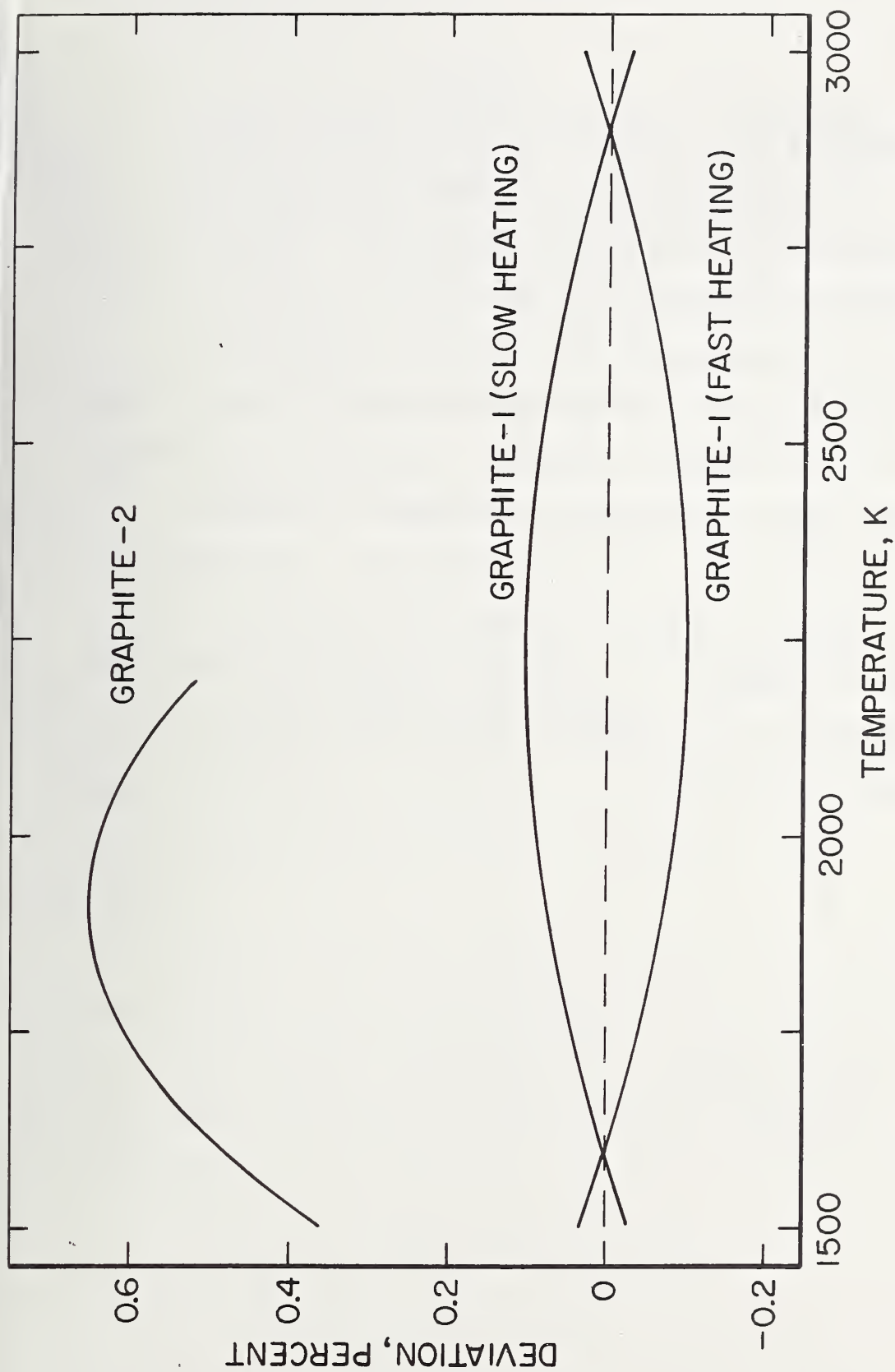


Figure 2. Deviation of smoothed heat capacity results for graphite-1 and graphite-2 from Equation (1).

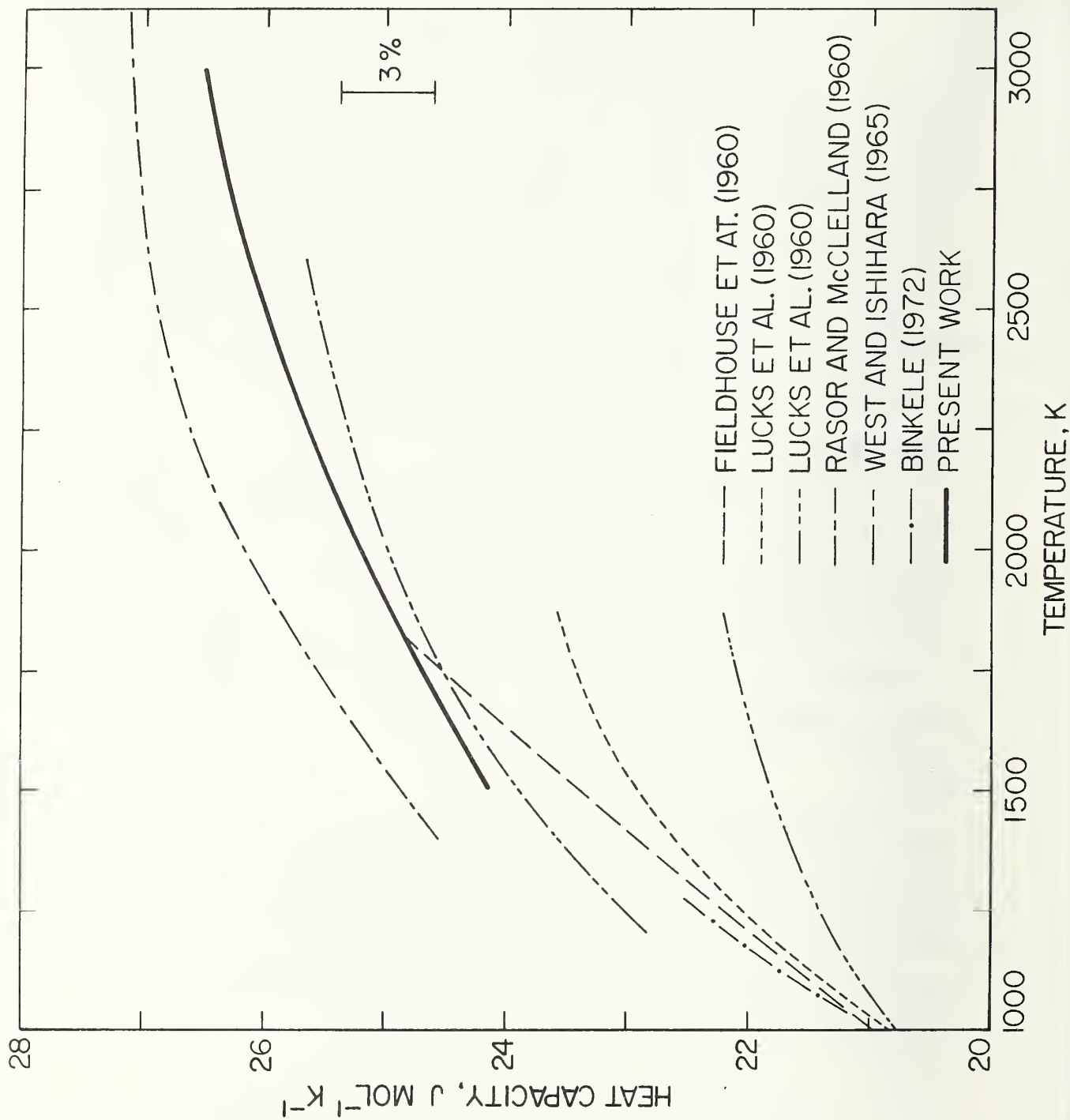
to be not more than 3%. To ensure the validity of this estimate, experiments were performed utilizing two different heating rates. At the highest temperature (3000 K), heat loss in the "fast" and "slow" heating cases amounted to 26% and 45% of the input power, respectively. This corresponds to a difference of approximately 20% in radiation loss. In this case, an error of 3% in the measured heat loss would have amounted to a difference of approximately 0.6% in heat capacity obtained for the experiments corresponding to the two heating rates. Yet, in the present work, this difference is 0.1%. Therefore, in spite of the fact that heat loss by thermal radiation constitutes a large fraction of the input power, an accurate account of its magnitude has not affected the accuracy of the heat capacity results.

## DISCUSSION

Heat capacity results obtained for the two graphite specimens under different experimental conditions were reproducible and internally consistent. Electrical resistance measurements (with a Kelvin bridge) before and after the pulse experiments were in agreement within 0.1%, which indicates that no significant structural or chemical changes had taken place in the specimen as the result of its heating to high temperatures. It may be concluded that the graphite specimens used in this work were stable under the present operating conditions.

Only a limited number of experimental results for graphite are available in the literature at temperatures above 1500 K. Since most of them are for different grades of graphite, it is difficult to have a common ground for comparison. As it may be seen in Figure 3, considerable differences exist between the results of various investigators.

The results of the present work agrees best with those reported by West and Ishihara [5] on grade CCH graphite. In the temperature range from 1500 to 2000 K, the agreement is within 0.8%. However, the difference increases with increasing temperature, amounting to 1.7% at 2600 K.



The curve (in Figure 3) showing the results of Rasor and McClelland [6] is an average, as given by the authors, representing data on four grades of graphite (3474D, 7087, GBH, and GBE). Actual data have a scatter of approximately 5% about the smooth curve. The difference between the results of Rasor and McClelland and those of the present work is, on the average, approximately 3%.

Lucks et al. [7] have reported results for two grades of graphite. The upper and lower curves (in Figure 3) represent the results for the grades 7087 and GBH, respectively. The disagreement between the results of Lucks et al. and Rasor and McClelland for the same grades of graphite is more than 10%.

Over the overlapping temperature region (1500 to 1800 K), the results for ATJ graphite reported by Fieldhouse et al. [8] agree, within 3%, with those of the present work. However, the slope of the curve representing the results of Fieldhouse et al. is considerably greater than that of the present work.

In addition to the present measurements, the only other known measurement on the same grade of graphite was performed by Binkle [9]<sup>6</sup> in the temperature range from 373 to 1273 K. Since there is no overlapping region, it is difficult to report the differences in the two results. However, from Figure 3 it may be seen that an extrapolation of Binkle's results to 1500 K is likely to yield a value approximately 2% lower than that of the present work.

---

<sup>6</sup>The graphite (AXM-5Q, Poco) specimen used by Binkle was also furnished by the U. S. Air Force Materials Laboratory.

The rather close agreement between the results of West and Ishihara [5] and those of the present work, which were obtained on two different grades of graphite using two different measurement techniques, indicates that heat capacity of graphite may not be very sensitive to differences in the grades, at least for some of the grades. Therefore, the differences in the literature results should not be entirely attributed to grade differences, as it is likely that these differences might have been mostly due to experimental errors. In addition, the state of the specimen (purity, degree of graphitization and annealing) undoubtedly plays an important role in the results. A final conclusion regarding heat capacity of graphite can only be reached after performing additional accurate measurements on other grades of graphite.

It may be seen that the heat capacity of graphite reaches the Dulong and Petit value of  $3R$  ( $24.943 \text{ J mol}^{-1}\text{K}^{-1}$ ) at approximately 1850 K, and continues to increase above that temperature.

The rate of change of heat capacity with temperature decreases from a value of  $2.5 \times 10^{-3} \text{ J mol}^{-1}\text{K}^{-2}$  at 1500 K to a value of  $6.8 \times 10^{-4} \text{ J mol}^{-1}\text{K}^{-2}$  at 3000 K. This rather unusual trend for heat capacity at high temperatures (above 1500 K) is due to the high value of the Debye temperature (1550 K [10]) for graphite.

Future heat capacity measurements at temperatures above 3000 K promise to yield information of practical and theoretical significance. It is important to resolve the question whether heat capacity of graphite reaches a constant value at temperatures above approximately 3300 K, or increases sharply above this temperature, as was reported by Rasor and McClelland [6].

In summary, the two potentially useful research areas in connection with the heat capacity of graphite are:

(1) Investigations of the dependence of heat capacity on graphite grades, and graphite stability from the viewpoint of reproducibility of heat capacity measurements at temperatures below 3000 K.

(2) Accurate measurements in the range 3000 K to the sublimation point of graphite. These measurements have to be performed with the specimen in a pressurized environment to suppress evaporation.

#### ACKNOWLEDGEMENT

The author expresses his gratitude to Dr. C. W. Beckett for his continued interest and encouragement of research in high-speed methods of measuring thermophysical properties. The contribution of Mr. M. S. Morse in connection with electronic instrumentation is also greatly appreciated.

## REFERENCES

- [1] Foley, G. M., "High-Speed Optical Pyrometer", Rev. Sci. Instr., Vol. 41, 1970, pp. 827-834.
- [2] Cezairliyan, A., "Design and Operational Characteristics of a High-Speed (Millisecond) System for the Measurement of Thermophysical Properties at High Temperatures", J. Res. Nat. Bur. Stand. (U. S.), Vol. 75C (Eng. and Instr.), 1971, pp. 7-18.
- [3] Cezairliyan, A., M. S. Morse, H. A. Berman, and C. W. Beckett, "High-Speed (Subsecond) Measurement of Heat Capacity, Electrical Resistivity, and Thermal Radiation Properties of Molybdenum in the Range 1900 to 2800 K", J. Res. Nat. Bur. Stand. (U. S.), Vol. 74A (Phys. and Chem.), 1970, pp. 65-92.
- [4] International Practical Temperature Scale of 1968, Metrologia, Vol. 5, 1969, pp. 35-44.
- [5] West, E. D., and Ishihara, S., "A Calorimetric Determination of the Enthalpy of Graphite from 1200 to 2600 K", Advances in Thermophysical Properties at Extreme Temperatures and Pressures, Am. Soc. Mech. Eng., New York, 1965, pp. 146-151.
- [6] Rasor, N. S., and McClelland, J. D., "Thermal Properties of Graphite, Molybdenum, and Tantalum to Their Destruction Temperatures", J. Phys. Chem. Solids, Vol. 15, 1960, pp. 17-26.

- [7] Lucks, C. F., Deem, H. W., and Wood, W. D., "Thermal Properties of Six Glasses and Two Graphites", Am. Cer. Soc. Bull., Vol. 39, 1960, pp. 313-319.
- [8] Fieldhouse, I. B., Lang, J. I., and Blau, H. H., WADC TR 59-744, 1960, pp. 1-78, [AD 249 166].
- [9] Binkele, L., Private Communication, 1972.
- [10] Gschneidner, K. A., "Physical Properties and Interrelationships of Metallic and Semimetallic Elements", Solid State Physics, F. Seitz, and D. Turnbull, eds., Vol. 16, Academic Press, New York, 1965, pp. 275-426.

81186

### Chapter 3

#### THERMODYNAMIC FUNCTIONS FOR $\text{MoF}_5(\text{g})$

Thomas B. Douglas, Ralph F. Krause, Jr.,  
Nicolo Acquista, and Stanley Abramowitz

In last year's report two of us reported in detail the results of infrared and Raman spectroscopic investigations of  $\text{MoF}_5$  [1]. The structural and vibrational assignment of the molecule as stated there were not entirely complete and unambiguous for the purpose of generating a table of thermodynamic functions, but such an assignment of fundamentals was provided later [2], and led to the table computed and reported in the present chapter.

Ideal-gas thermodynamic functions for  $\text{MoF}_5$  gas (the monomer species) over the temperature range 0 to 6000 K are given in Table 1 in terms of the thermochemical calorie ( $=4.1840$  J) as the unit of energy, and in the format of the first five columns of the JANAF thermochemical tables [3]. (In " $H_{298}^\circ$ " the subscript refers to 298.15 K. The standard enthalpies and Gibbs energies of formation are not included because a reliable value for the heat of formation was not available, although it may be soon (Ref. [5], Chapters 5 and 6). Table 1 is repeated in Table 2 except with the joule as the unit of energy.) The harmonic-oscillator rigid-rotor approximation was used. The space group and vibrational fundamentals assumed are those referred to above [2]. The two fundamentals estimated but not observed are bracketed below, according to the usual custom. The Mo-F bond distances in the  $\text{MoF}_5$  molecule were assumed to be all the same, and to be equal to

the value found in an electron-diffraction study of  $\text{MoF}_6$  [4] and adopted in the JANAF table for that gas [3]. These tables for  $\text{MoF}_5$  assume a single electronic state, and a multiplicity of 2 to account for the known fact that  $\text{MoF}_5$  is electronically an "odd" molecule.

A collection of the molecular constants on which Tables 1 and 2 are based is as follows. The symbols have the same meanings as in the JANAF tables [3].

MOLYBDENUM PENTAFLUORIDE ( $\text{MoF}_5$ ) (IDEAL GAS) GFW = 190.932

Point Group [ $D_{3h}$ ]

$S_{298.15}^\circ = [82.4]$  gibbs/mol

Ground State Quantum Weight = [2]

#### Vibrational Frequencies and Degeneracies

$\omega, \text{cm}^{-1}$	$\omega, \text{cm}^{-1}$
759(1)	713(2)
738(1)	261(2)
683 (1)	112(2)
[500](1)	[200](2)

#### Electronic Levels and Quantum Weights

$\epsilon_i, \text{cm}^{-1}$	$g_i$
0	[2]

Bond Distance:  $\text{Mo-F} = [1.84] \text{ \AA}$

Bond Angles: [ $\text{F}^*-\text{Mo}-\text{F}^* = 120^\circ$   $\text{F}^*-\text{Mo}-\text{F}^{**} = 90^\circ$   $\text{F}^{**}-\text{Mo}-\text{F}^{**} = 180^\circ$ ]

\* Equatorial

\*\*Axial

$\sigma = [6]$

Product of the Moments of Inertia:  $I_A I_B I_C = [4.478 \times 10^{-113}] \text{ g}^3 \text{ cm}^6$

## REFERENCES

- [1] N. Acquista and S. Abramowitz, AFOSR Scientific Report AFOSR-TR-72-2004 (NBS Report 10904), National Bureau of Standards, Washington, D. C. 20234, July 1972, Chapter 3 (pp. 49-63).
- [2] S. Abramowitz (Dec. 5, 1972).
- [3] JANAF Thermochemical Tables, D. R. Stull and H. Prophet, Project Directors, 2nd ed., NSRDS-NBS 37, U. S. Government Printing Office, Washington, D. C. (June 1971).
- [4] G. M. Nazarian, Ph.D. Thesis, California Institute of Technology, Pasadena, Calif. (1957).
- [5] Report NBSIR 73-281, National Bureau of Standards, Washington, D. C. 20234 (AFOSR Agreement ISSA-73-0001), 1 July 1973.

Table 1. Ideal-Gas Thermodynamic Functions for Molybdenum Pentafluoride Monomer (MoF<sub>5</sub>)(in CALORIE<sup>a</sup> energy units)

T	C <sub>P</sub> <sup>o</sup>	S <sup>o</sup>	-(G <sup>o</sup> -H <sub>298</sub> <sup>o</sup> )/T	H <sup>o</sup> -H <sub>298</sub> <sup>o</sup>
K	cal mol <sup>-1</sup> K <sup>-1</sup>	cal mol <sup>-1</sup> K <sup>-1</sup>	cal mol <sup>-1</sup> K <sup>-1</sup>	kcal mol <sup>-1</sup>
.000	.000	.000	∞	-5.028
100.000	14.730	62.230	101.900	-3.968
200.000	20.319	74.204	85.260	-2.197
298.150	24.195	83.170	83.170	.000
300.000	24.254	83.320	83.170	.045
400.000	26.735	90.666	84.155	2.605
500.000	28.248	96.808	86.089	5.360
600.000	29.200	102.049	88.323	8.236
700.000	29.825	106.600	90.616	11.189
800.000	30.254	110.612	92.870	14.194
900.000	30.559	114.104	95.044	17.236
1000.000	30.783	117.426	97.123	20.303
1100.000	30.951	120.368	99.104	23.390
1200.000	31.082	123.067	100.990	26.492
1300.000	31.184	125.559	102.786	29.606
1400.000	31.266	127.873	104.496	32.728
1500.000	31.333	130.033	106.127	35.858
1600.000	31.388	132.057	107.685	38.995
1700.000	31.434	133.961	109.176	42.136
1800.000	31.472	135.759	110.603	45.281
1900.000	31.505	137.462	111.972	48.430
2000.000	31.533	139.078	113.287	51.582
2100.000	31.557	140.617	114.552	54.736
2200.000	31.578	142.086	115.771	57.893
2300.000	31.596	143.490	116.946	61.052
2400.000	31.612	144.835	118.080	64.212
2500.000	31.626	146.126	119.176	67.374
2600.000	31.639	147.366	120.237	70.537
2700.000	31.650	148.561	121.264	73.702
2800.000	31.660	149.712	122.259	76.867
2900.000	31.669	150.823	123.225	80.034
3000.000	31.677	151.897	124.163	83.201
3100.000	31.685	152.936	125.075	86.360
3200.000	31.692	153.942	125.961	89.538
3300.000	31.698	154.917	126.824	92.707
3400.000	31.703	155.863	127.664	95.877
3500.000	31.708	156.782	128.483	99.048
3600.000	31.713	157.676	129.282	102.219
3700.000	31.717	158.545	130.061	105.391
3800.000	31.721	159.391	130.822	108.563
3900.000	31.725	160.215	131.565	111.735
4000.000	31.729	161.018	132.291	114.908
4100.000	31.732	161.801	133.001	118.081
4200.000	31.735	162.566	133.696	121.254
4300.000	31.737	163.313	134.376	124.428
4400.000	31.740	164.043	135.042	127.601
4500.000	31.742	164.756	135.695	130.776
4600.000	31.745	165.454	136.334	133.950
4700.000	31.747	166.136	136.961	137.124
4800.000	31.749	166.805	137.576	140.299
4900.000	31.751	167.459	138.179	143.474
5000.000	31.752	168.101	138.771	146.649
5100.000	31.754	168.730	139.352	149.825
5200.000	31.755	169.346	139.923	153.000
5300.000	31.757	169.951	140.484	156.176
5400.000	31.758	170.545	141.035	159.351
5500.000	31.760	171.127	141.577	162.527
5600.000	31.761	171.700	142.110	165.703
5700.000	31.762	172.262	142.634	168.880
5800.000	31.763	172.814	143.149	172.056
5900.000	31.764	173.357	143.657	175.232
6000.000	31.765	173.891	144.156	178.409

<sup>a</sup> 1 cal = 4.1840 J

Table 2. Ideal-Gas Thermodynamic Functions for Molybdenum Pentafluoride Monomer (MoF<sub>5</sub>)  
(in JOULE energy units)

T	C <sub>p</sub> <sup>o</sup>	S <sup>o</sup>	-(G <sup>o</sup> -H <sub>298</sub> <sup>o</sup> )/T	H <sup>o</sup> -H <sub>298</sub> <sup>o</sup>
K	J mol <sup>-1</sup> K <sup>-1</sup>	J mol <sup>-1</sup> K <sup>-1</sup>	J mol <sup>-1</sup> K <sup>-1</sup>	kJ mol <sup>-1</sup>
.000	.000	.000	∞	-21.037
100.000	61.631	260.369	426.389	-16.602
200.000	85.015	310.802	356.765	-9.193
298.150	101.234	347.982	347.982	.000
300.000	101.478	348.609	347.984	.188
400.000	111.861	379.348	352.104	10.897
500.000	118.190	405.045	360.195	22.425
600.000	122.171	425.973	369.543	34.458
700.000	124.787	446.015	379.137	46.815
800.000	126.581	462.802	388.567	59.388
900.000	127.857	477.749	397.663	72.114
1000.000	128.794	491.311	406.363	84.948
1100.000	129.501	503.621	414.653	97.865
1200.000	130.046	514.914	422.544	110.843
1300.000	130.475	525.340	430.056	123.870
1400.000	130.818	535.023	437.212	136.935
1500.000	131.097	544.058	444.037	150.032
1600.000	131.327	552.526	450.556	163.153
1700.000	131.518	560.494	456.791	176.296
1800.000	131.679	568.016	462.763	189.456
1900.000	131.815	575.139	468.492	202.631
2000.000	131.932	581.903	473.994	215.818
2100.000	132.033	588.343	479.287	229.016
2200.000	132.121	594.487	484.385	242.224
2300.000	132.197	600.362	489.301	255.440
2400.000	132.264	605.990	494.047	268.663
2500.000	132.324	611.390	498.633	281.893
2600.000	132.377	616.581	503.070	295.128
2700.000	132.424	621.578	507.368	308.368
2800.000	132.466	626.395	511.533	321.612
2900.000	132.504	631.044	515.574	334.861
3000.000	132.538	635.536	519.490	348.113
3100.000	132.569	639.883	523.312	361.369
3200.000	132.597	644.092	527.021	374.627
3300.000	132.623	648.173	530.631	387.888
3400.000	132.646	652.132	534.147	401.151
3500.000	132.668	655.978	537.573	414.417
3600.000	132.687	659.715	540.914	427.685
3700.000	132.706	663.351	544.174	440.955
3800.000	132.722	666.890	547.357	454.226
3900.000	132.738	670.338	550.467	467.499
4000.000	132.752	673.699	553.506	480.773
4100.000	132.765	676.977	556.477	494.049
4200.000	132.778	680.177	559.384	507.327
4300.000	132.789	683.301	562.230	520.605
4400.000	132.800	686.354	565.017	533.884
4500.000	132.810	689.338	567.746	547.165
4600.000	132.819	692.257	570.421	560.446
4700.000	132.828	695.114	573.044	573.729
4800.000	132.836	697.911	575.616	587.012
4900.000	132.844	700.650	578.140	600.296
5000.000	132.852	703.334	580.617	613.581
5100.000	132.858	705.964	583.049	626.866
5200.000	132.865	708.544	585.438	640.152
5300.000	132.871	711.075	587.785	653.439
5400.000	132.877	713.559	590.091	666.727
5500.000	132.882	715.997	592.358	680.015
5600.000	132.887	718.392	594.587	693.303
5700.000	132.892	720.744	596.780	706.592
5800.000	132.897	723.055	598.937	719.882
5900.000	132.901	725.327	601.060	733.171
6000.000	132.906	727.561	603.150	746.462

(81187)

ALTERNATIVE PROCEDURES IN INTERPRETING EQUILIBRIUM DATA ON  
PARTIALLY ASSOCIATED VAPORS

by Thomas B. Douglas and Ralph F. Krause, Jr.

Abstract

Alternative classical-thermodynamic and quasi-chemical treatments applicable to equilibrium data of various types on vapors composed of many species representing various degrees of association are discussed at some length. An example unexpectedly giving ambiguous mathematical solutions is presented. A computation illustrates the sensitivity of derived thermodynamic properties to errors in the individual data.

As mentioned in the Introduction to a chapter of another report [5], our earlier data for the vapor pressure of liquid  $\text{MoF}_5$ , when combined with our transpiration data on the same substance, had led us to believe that the saturated vapor must contain (in the temperature range of our measurements) numerous species in appreciable amounts and representing different degrees of molecular association. As a result we examined and developed several alternative procedures for deriving meaningful thermodynamic properties from a limited set of data on such a vapor. While our most recent vapor-pressure data for  $\text{MoF}_5$  suggest a much smaller degree of association [5] and hence less urgency to use elaborate procedures of interpretation, we set

forth in this chapter the more significant aspects of this mathematical exploration in the belief that they may contribute helpfully to dealing with other vapors that are actually associated in such a complex way.

### I. A Classical-Thermodynamic Interpretation

This type of approach applies rigorously to the case of two or more molecular species in the vapor in major proportions (formally evidenced by the fact that simple relations such as the ideal-gas law do not or may not hold to a sufficient approximation), but ignores the existence of all such species and treats the vapor as a single substance. In the resulting equations, all extensive quantities (V, volume; H, enthalpy; etc.) refer to a defined amount of the substance or phase in question (unit mass could be selected, but we shall choose instead a "mole" defined as a gram-formula-weight in terms of the monomer formula). These facts may seem too elementary to mention, but are sometimes almost forgotten, so strong is the present-day vogue of describing the properties of a vapor in terms of those of its actual or supposed ideal components.

We limit ourselves here to a consideration of the three types of measurements which we have undertaken on  $\text{MoF}_5$ : (a) The true vapor pressure ("A") at absolute temperature T; (b) the apparent vapor pressure ("B") at T, from transpiration and assumption of the ideal-gas law using the defined mole; and (c) the pressure of the

unsaturated vapor at T produced by heating vapor, at constant volume, from a lower temperature T' where it was saturated. (The unsaturated vapor is of course bivariant: T specifies its temperature, and T' is equivalent to specifying its volume or density, so that in principle the complete set {T, T'} covers all possible states of unsaturated vapor.)

Using V for the molar vapor volume and subscript "sat" for saturated conditions of liquid-vapor equilibrium, we can then write

$$A = P_{\text{sat}}; \quad (1)$$

$$B = RT/V_{\text{sat}}. \quad (2)$$

Since the gas is not ideal (experimentally,  $B > A$ ), one cannot use for conditions of vaporization equilibrium the Clausius-Clapeyron equation, but may use its parent, the (exact) Clapeyron equation, which is, omitting the usually negligible liquid volume,

$$(\partial P / \partial T)_{\text{sat}} = \Delta H^{\text{vap}} / TV. \quad (3)$$

Substituting from Eqs. (1) and (2),

$$\Delta H^{\text{vap}} = (RT^2/B) (dA/dT). \quad (4)$$

Equation (4) gives the heat of vaporization to form a defined mole of saturated vapor. For the vapor in question, unlike an ideal gas, the enthalpy and hence the heat of vaporization depend on the pressure (or volume) of the vapor as well as on temperature, and this

variation can be expressed by the exact thermodynamic relation

$$(\partial H/\partial P)_T = V - T(\partial V/\partial T)_P. \quad (5)$$

From the mathematical identity for continuous functions

$$(\partial V/\partial T)_P = -(\partial P/\partial T)_V/(\partial P/\partial V)_T \quad (6)$$

Eq. (5) becomes

$$(\partial H/\partial P)_T = V + T (\partial P/\partial T)_V/(\partial P/\partial V)_T. \quad (7)$$

Application of Eq. (7) over a finite pressure (or volume) range at, say, temperature  $T$  requires enough data to allow integration of the right-hand side from the saturated state to lower pressures. These data would in principle be provided by experiments of Type (c) mentioned above, with data for various temperature  $T'$  (up to  $T$ ), and also some variation in Temperature  $T$  to evaluate  $(\partial P/\partial T)_V$ .

Other thermodynamic properties could be similarly derived, but will not be given.

In the subsequent sections of this chapter, procedures are outlined for interpreting the data on the assumption that the vapor behaves as a mixture of ideal-gas species whose properties admit of some degree of quantitative discrimination. In contrast, the classical-thermodynamic approach may have the advantage of being less presumptuous; on the other hand, it affords less scientific insight into the molecular structure of the vapor (often useful in comparing and correlating different chemical compounds of a series), and it runs the risk that if the results are extrapolated to widely different

conditions, they may fail to reflect changing trends that occur in the real system owing to the accentuation or suppression of specific molecular species.

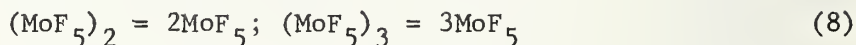
## II. Quasi-Chemical Interpretations

The commonly used term "quasi-chemical" to describe a vapor or other fluid as a mixture of two or more molecular species in chemical equilibrium seems like a wisely chosen one, particularly when (as we do here) the species are assumed to behave ideally. That the model is at least somewhat arbitrary is well illustrated by the vigorous effort many decades ago to define the molecular species of liquids in such a way that in terms of these species their properties were those of "ideal" mixtures; but invariably this led to inconsistencies traceable to treating two physically adjacent "molecules" as a single molecule under some conditions but as two separate molecules under other conditions. Nevertheless, the model appears to be an excellent one for low-density vapors (such as that of  $\text{MoF}_5$  in the temperature range of the present investigation), and mass and absorption spectroscopy have voluminously supported this idea in recent years.

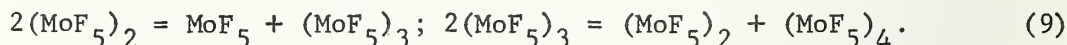
### II 1. Preliminary: A Combination of Data Yielding Ambiguous Thermodynamic Solutions

As is usually the case, the infrared and Raman spectroscopy on  $\text{MoF}_5$  vapor [1] yielded some bands attributed to the monomer and others attributed to associated molecules, but the vibrational modes are much too complicated to allow identification of the different

species (except the monomer) or their properties with any reliability. The mass-spectrometric behavior is, of course, far simpler to interpret, and there have been two such investigations of  $\text{MoF}_5$  vapor of which we are aware [2, 3]. Collectively speaking, these two mass-spectrometric researches detected in low-pressure  $\text{MoF}_5$  vapors the four species  $(\text{MoF}_5)_n$  with  $n = 1-4$ , and led at stated temperatures to heats of the two reactions



and to species proportions which seemingly can be used with the greatest cancellation of experimental error to express the (pressure-independent) equilibrium constants of two independent "isomolecular" reactions which may be taken to be:



Our first serious attempt to develop a general interpretation of the emerging assembly of data for  $\text{MoF}_5$  vapor was to assume only these four species and to write a general computer program (actually, two alternate programs were written independently) that would take as input data from zero to three data (with accompanying temperatures, which could all differ) of each of five types: (a), (b), and (c) of Section I; heats of one or both reactions of Eq. (8); and equilibrium constants for one or both reactions of Eq. (9). After assuming what are sufficiently accurate " $\Delta C_p$ " coefficients, each program was capable of computing the remaining two constants in each  $\ln P$ -vs.- $T$  equation

for the four vaporization reactions  $n \text{ MoF}_5(l) = (\text{MoF}_5)_n(g)$ . Thus each program generated eight constants, and in a single run was designed to use just eight data of the types enumerated (without weighting or "least-squaring"). Our long-range purpose was to evaluate a set of thermodynamic parameters which would reflect our data and the mass-spectroscopic data with judicious weighting. Our immediate goal was to be able to plan our future measurements with least propagation of experimental error into the thermodynamic parameters calculated from the data.

Each program was tested and found completely accurate. With combinations of data for  $\text{MoF}_5$  (some very roughly estimated) as input, the eight constants generated were shown beyond doubt to always reproduce the input data exactly. Since the equations are non-linear, such a program expands them linearly around an initial (approximate) solution, and one might suppose that of the many real mathematical solutions for any given data set, one can assume that only one solution is physically possible (i.e., all partial pressures positive in this case). This proved not to be true! As verified by both programs, a single data set was found to give two very substantially different solutions depending on which of two initial solutions was used, but not depending on which computer program was employed. We were thus alerted to the fact that the data input for this type of program is too general to guarantee a unique solution for the thermodynamic properties of the different species. Solutions of such computations should of course be examined for uniqueness before being accepted.

Numerical details of these computations are not given here because, aside from the ambiguity just discussed, the input data were too uncertain and subject to magnified error propagation as illustrated later (Section II 3).

## II 2. Using Only Two Independent Data for Each Temperature

The mass-spectrographic data for  $\text{MoF}_5$  vapor [2, 3] indicate proportions of species which are distinctly smaller the higher the degree of association. But, of course, the proportions of the higher species increase in a predictable way as one isothermally increases the total pressure toward saturation, which is the state for most of our data. In fact, the calculations outlined in the preceding section led us to suspect at first that for saturated  $\text{MoF}_5$  vapor in the temperature range of our measurements the abundance does not fall off enough in going from monomer to tetramer to justify neglecting all still higher species (pentamer, hexamer, etc.). Accordingly, we decided that a more realistic approach was to assume an infinite number of vapor species  $(\text{MoF}_5)_n$  ( $n = 1$  to  $\infty$ ), but to assume enough reasonable relations among the different species to leave undetermined a number of parameters equal to the number of independent data used (this number differing in this and the next section). This procedure will oversimplify the relations among the higher species; but since in many cases they are minor individually but appreciable collectively, this essentially lumps them together in a plausible way instead of ignoring them entirely. The procedure is highly analogous to our treatment of vaporization data for the  $\text{AlF}_3$ - $\text{AlCl}_3$  system [4], where we undertook to assign the equivalent of two thermodynamic parameters to each of 28 gas species on the basis of a far smaller number of data.

A further modification of the approaches of this and the next section, compared with the preceding section, is to treat the data for each temperature independently, as this proves to afford simpler criteria for ascertaining that a given set of data will yield a unique solution for the thermodynamic parameters of the vapor species.

In line with the discussion above, we assumed the vapor to be composed of ideal-gas species which in the case of  $\text{MoF}_5$  vapor are  $(\text{MoF}_5)_n$  with  $n$  varying from 1 to  $\infty$ , and we shall assume as data at a given temperature the total vapor pressure  $A$ , and the apparent vapor pressure  $B$  calculated from transpiration assuming the monomer ( $m = 1$ ) molecular weight. Using  $P_n$  for the partial pressure of Species  $\underline{n}$  and remembering that the transpiration data measure the available number of monomer units, we have (the summation " $\Sigma$ " extending over all values of  $n$  from 1 to  $\infty$ )

$$\Sigma P_n = A; \quad (10)$$

$$\Sigma n P_n = B. \quad (11)$$

Now we assume a ratio  $q$ , defined by

$$q \equiv P_{n+1}/P_n \quad (12)$$

and to be determined from the data, to depend on temperature but not  $\underline{n}$ , with

$$0 \leq q < 1. \quad (13)$$

using Eq. (12) to eliminate all  $P_n$ 's except  $P_1$ , Eqs. (10) and (11)

give

$$P_1 (1 + q + q^2 + \dots) = P_1 / (1 - q) = A; \quad (14)$$

$$P_1 (1 + 2q + 3q^2 + \dots) = P_1 / (1 - q)^2 = B. \quad (15)$$

From Eqs. (14) and (15)

$$q = 1 - (A/B); \quad (16)$$

$$P_1 = A^2 / B \quad (17)$$

and in general

$$P_n = [A^2 / (B - A)] [(B - A) / B]^n. \quad (18)$$

The values and temperature coefficients of the  $P_n$ 's determine values for the equilibria and heats of the various vaporization and all-gas reactions, using the usual thermodynamic relations.

It is clear from Eq. (18) that specific values of A and B give a unique value for each  $P_n$  (and for every other thermodynamic parameter derived therefrom). Furthermore, the sensitivity of each  $P_n$  to experimental errors in A and B is not ordinarily great, and can readily be determined from Eq. (18).

This simple treatment, unlike either type of data (A or B) alone, promises to give a measure of the degree of saturated-vapor association and its change with temperature, and the results would be accurate if the saturated vapor were composed of just two ideal species, and satisfactory if the vapor were mainly one species which is only slightly associated or dissociated. However, we may examine some of the consequences of the above treatment, and see whether

the available data are consistent with them. We immediately find that Eq. (18) predicts unity at every temperature for the equilibrium constant of every "isomolecular" all-gas reaction such as those of Eq. (9) (Section II 1), and as a further consequence, a heat (or  $\Delta H$ ) for such a reaction that is essentially zero. The available mass-spectrographic data for  $\text{MoF}_5$  vapor [2, 3], even if only roughly accurate, are at variance with these conclusions. The next section suggests a reason why  $\text{MoF}_5$  vapor may behave anomalously in that sense, and develops a modified treatment designed to overcome this objection for substances of that type.

### II 3. Using Three Independent Data for Each Temperature

We again assume the infinite number of ideal-gas species illustrated by  $(\text{MoF}_5)_n$  with  $n$  from 1 to  $\infty$ . As experimental data we assume (all at absolute temperature  $T$  unless otherwise specified) not only  $A$  and  $B$  [defined by Eqs. (10) and (11)] but also data corresponding to one unsaturated state at  $T$  corresponding to Type (c) described early in Section I. Limiting " $P_n$ " to the saturated vapor and using " $p_n$ " for the unsaturated vapor, we define for vapor at  $T$  that at the same volume was saturated at  $T'$

$$\sum p_n \equiv D; \quad (19)$$

$$(T/T')(\sum n P_n)_{T'} \equiv C. \quad (20)$$

Four independent equations will be developed to use the data  $A$ ,  $B$ ,  $C$ , and  $D$ .

In addition to the parameter  $P_1$ , it is convenient to define three additional parameters ( $R_2$ ,  $R_3$ , and  $r_1$ ) as follows:

$$P_2/P_1 \equiv R_2 \quad (21)$$

$$P_{n+2}/P_n \equiv R_3 \quad (22)$$

$$P_1/P_1 \equiv r_1 \quad (23)$$

with possible ranges

$$0 \leq R_3 < 1 \quad (24)$$

$$0 \leq R_2 \leq \infty \quad (25)$$

$$0 \leq r_1 \leq 1 \quad (26)$$

Then for the saturated-vapor species pressures (relative to  $P_1$ ) we have an odd and an even series:

<u>n odd:</u>	<u>n even</u>	
$P_1/P_1 = 1$	$P_2/P_1 = R_2$	} (27)
$P_3/P_1 = R_3$	$P_4/P_1 = R_2 R_3$	
$P_5/P_1 = R_3^2$	$P_6/P_1 = R_2 R_3^2$	
.....	.....	
$P_n/P_1 = R_3^{(n-1)/2}$	$P_n/P_1 = R_2 R_3^{(n-2)/2}$	

(As special cases, if  $R_2 = 0$  we have only odd species; and if  $R_2 = \infty$ , we have only even species.) The species partial pressures in the unsaturated vapor can be obtained readily from the isothermal

invariance of an equilibrium constant--e.g.,

$$p_n/p_1^n = P_n/P_1^n. \quad (28)$$

Substitution for  $p_1$  from Eq. (23) and for  $P_n$  from Eqs. (27) gives

$$\left. \begin{array}{l} n \text{ odd: } p_n = (P_1 r_1)(R_3 r_1^2)^{(n-1)/2} \\ n \text{ even: } p_n = (R_2 P_1 r_1^2)(R_3 r_1^2)^{(n-2)/2} \end{array} \right\} \quad (29)$$

The "odd" species  $(\text{MoF}_5)_n$  (where  $n$  is odd) each have an odd number of electrons, so that one electron (at least) must be unpaired; but each "even" species has an even number of electrons and one may postulate the simplest case of no unpaired electrons. With few exceptions<sup>3</sup>, odd molecules show a decided tendency to associate, presumably through a tendency to decrease the number of free electrons. We may examine four general association reactions in the  $\text{MoF}_5$  system, and formulate their equilibrium constants from Eqs. (27), as follows.

Reaction	$n$	$\Delta(\text{no. of unpaired electrons})$	$K_P$
$(\text{MoF}_5)_{n-2} + (\text{MoF}_5)_2 = (\text{MoF}_5)_n$	odd	0	$R_3/R_2 P_1$
	even	0	
$(\text{MoF}_5)_{n-1} + (\text{MoF}_5)_1 = (\text{MoF}_5)_n$	odd	0	$R_2/P_1$
	even	-2	

In this section (as not in Section II 2)  $R_3 \neq R_2^2$ , so as a consequence the equilibrium constant (and  $\Delta H$ ) is allowed to reflect a net change in the number of unpaired electrons. (Because of the latter, we would expect an extra loss of entropy in the fourth reaction above, but in its equilibrium constant this may be more than counterbalanced at ordinary temperatures by an extra loss of energy.)

<sup>3</sup>In a mass-spectrometric study [3]  $\text{CrF}_5$  was measured, but none of its associated species was detected.

When the individual  $P_n$ 's are substituted from Eqs. (27) into Eqs. (10) and (11) and the infinite series are replaced by their closed-bracket equivalents, we get

$$P_1 (1 + R_2)/(1-R_3) = A; \quad (30)$$

$$P_1 (1 + 2 R_2 + R_3)/(1-R_3)^2 = B. \quad (31)$$

Owing to the same volume at  $T'$  and  $T$  and the assumption of ideal-gas species, it can be shown that at  $T$

$$\sum n p_n = C. \quad (32)$$

On substituting for the  $p_n$ 's from Eqs. (29) into Eqs. (19) and (32), one obtains

$$P_1 r_1 (1 + R_2 r_1)/(1-R_3 r_1^2) = D; \quad (33)$$

$$P_1 r_1 (1 + 2R_2 r_1 + R_3 r_1^2)/(1-R_3 r_1^2)^2 = C. \quad (34)$$

Using data  $A$ ,  $B$ ,  $C$ , and  $D$  for a given temperature, Eqs. (30), (31), (33), and (34) may be solved simultaneously for the parameters  $P_1$ ,  $R_2$ ,  $R_3$ , and  $r_1$ , whose values substituted into Eqs. (27) and (29) give the partial pressure of each species in the saturated and unsaturated vapor, according to the present treatment.

Since these four equations are nonlinear in some of the parameters to be solved for, there are of course multiple solutions mathematically, and the solution accepted must of course indicate positive finite partial pressures for all species. For such an acceptable solution, the data must obey the relative order

$$B \geq A \geq D; B \geq C. \quad (35)$$

An attempt to prove generally that a data set obeying Eq. (35) gives only one "acceptable" solution was unsuccessful, owing to the simultaneous occurrence of several sign ambiguities in the equations examined. However, by a series of arguments that will not be repeated here, uniqueness of acceptable solution was proved for any data set in the neighborhood of the "representative" set presently used as an example.

A computer program was written to solve Eqs. (30), (31), (33), and (34) simultaneously (using linear expansion and iteration). As a specific example, the program was solved using a definite set of values for the "data" A, B, C, and D. The solution was then repeated four times, each time arbitrarily increasing one of the assumed data by 1%. The specific original data set was chosen partly to approximate preliminary experimental results for  $\text{MoF}_5$ . The results (some truncated) are given in Table 1, labeled for a vapor system  $X_n$  (lest someone be tempted to assume that they are trustworthy for  $(\text{MoF}_5)_n$ ). A comparison of the results of the five computer solutions should, however, provide some measure of the sensitivity to experimental errors of the vapor-species properties when calculated for typical cases as proposed in the present section. Furthermore, since the computer cost is negligible, such a program is useful in planning future measurements whose errors would produce the least serious effects.

An examination of the lower part of Table 1 shows that (at least in this example) a 1% error in a single datum leads to several percent

Table 1. An Example Illustrating the Errors in Calculated  
Partial Pressures and Proportions of Gas Species  $X_n$   
Resulting from Experimental Errors in the Input Data

[Equations (30), (31), (33), and (34) were used. The calculated values are for temperature T.  $P_n$  applies to the saturated vapor, and  $p_n$  to the unsaturated vapor.  $N_n \equiv P_n / \sum P_n$ .]

Original "Data" and Calculated Values (approximate)				
T = 392 K	C = 5.10 torr	$r_1 = 0.70$	$N_2 = 0.556$	
T' = 372 K	D = 2.62 torr	$P_1 = 1.094$ torr	$N_3 = 0.049$	
A = 5.63 torr	$R_2 = 2.86$	$p_1 = 0.766$ torr	$N_4 = 0.139$	
B = 13.55 torr	$R_3 = 0.25$	$N_1 = 0.194$	$N_1 + N_2 + N_3 + N_4 = 0.938$	

Percentage Changes in Calculated Parameters when One "Datum" is Assumed 1% Higher

Calculated Parameter	The Input "Datum" Assumed 1% Higher			
	A	B	C	D
$R_2$	+ 9.5	- 6.2	+ 12.6	- 13.0
$R_3$	- 4.7	+ 4.1	- 2.5	+ 3.1
$r_1$	- 0.6	+ 0.2	+ 0.2	+ 0.3
$P_1$	- 4.2	+ 3.4	- 7.8	+ 9.5
$P_2$	+ 4.9	- 3.0	+ 3.8	- 4.7
$P_3$	- 8.7	+ 7.6	- 10.1	+ 12.9
$P_4$	+ 0.03	+ 0.9	+ 1.2	- 1.8
$P_1$	- 4.8	+ 3.6	- 7.6	+ 9.8
$N_1$	- 5.1	+ 3.4	- 7.8	+ 9.5
$N_2$	+ 3.9	- 3.0	+ 3.9	- 4.7
$N_3$	- 9.6	+ 7.6	- 10.9	+ 12.9
$N_4$	- 1.0	+ 0.9	+ 1.2	- 1.8
$N_1 + N_2 + N_3 + N_4$	+ 0.6	- 0.6	+ 0.3	- 0.4

error in many of the more important parameters calculated. There will actually be errors, of course, in all the data. To the extent that these errors are random, the overall uncertainties will be somewhat magnified. However, the errors in A and C are seen to usually produce effects of opposite sign to those from errors in B and D, and since all four data are pressure determinations, the effects of systematic errors in pressure determination will tend to cancel more or less. Nevertheless, Table 1 suggests that a single-datum accuracy to 1% or better is probably necessary to obtain significant results by the procedure of this section, and that with a much higher inaccuracy (say, 5%) the use of this many independent measurements on the vapor would hardly be worthwhile. This would clearly be even more pointedly true were one to attempt measurements also on a second unsaturated vapor state (at the same temperature), in the hope of getting still more detailed information on the vapor.

### III. References

- [1] N. Acquista and S. Abramowitz, AFOSR Scientific Report AFOSR-TR-72-2004 (NBS Report 10904), National Bureau of Standards, Washington, D. C. 20234, July 1972, Chapter 3 (pp. 49-63).
- [2] C. F. Weaver and J. D. Redman, Section 11.6.3 of ORNL Report 4449, Oak Ridge, Tenn., Feb. 1970, p. 116.
- [3] W. E. Falconer, Bell Research Laboratories, Murray Hill, N. J., private communication (Sept. 1972).

- [4] R. F. Krause, Jr., and T. B. Douglas, J. Phys. Chem. 72, 3444-3451 (1968).
- [5] T. B. Douglas and R. F. Krause, Jr., "The Vapor-Pressure at 393 K of Liquid Molybdenum Pentafluoride, MoF<sub>5</sub>, According to Preliminary Static-Method Measurements," Chapter 6 of Report NBSIR 73-281, National Bureau of Standards, Washington, D. C. 20234 (AFOSR-ISSA-73-0001), 1 July 1973.

Chapter 5  
CHANGE IN NORMAL SPECTRAL EMITTANCE (AT 650 nm)  
OF NIOBIUM DURING MELTING AND  
ITS RELATION TO SURFACE ROUGHNESS\*

Ared Cezairliyan  
National Bureau of Standards  
Washington, D. C. 20234

The objective of this note is to report investigations on the behavior of the normal spectral emittance (at 650 nm) of niobium during melting. An attempt is made to relate the difference between the emittances of solid and liquid niobium at the melting point to the roughness of the solid surface.

The technique used for the measurements reported in this work is based on resistive self-heating of the specimen from room temperature to its melting point in less than one second, and measuring the specimen radiance temperature at the rate of 1200 times per second with a high-speed photoelectric pyrometer. The interference filter used for radiance temperature measurements had an effective wavelength of 650 nm and a bandwidth of 10 nm. The circular area viewed by the pyrometer was 0.2 mm in diameter. The construction and operation of the measurement system are described in earlier publications[1, 2]. The details of the experiments for radiance temperature measurements on the niobium specimens are given in another publication [3]. The niobium specimens (99.9<sup>+</sup> percent pure) were in the form of strips with the following nominal dimensions:

---

\*This work was supported in part by the U. S. Air Force Office of Scientific Research.

length 75 mm; width, 6.3 mm; and thickness, 0.25 mm. The results of radiance temperature measurements near and at the melting point for a typical case are shown in Figure 1. The plateau corresponds to melting of the specimen. The drop at the beginning of the plateau corresponds to the change in the normal spectral emittance of the specimen surface as it melts. An initial high radiance temperature (peak of spike) indicates that normal spectral emittance of the solid surface is higher than that of the liquid surface. The normal spectral emittances corresponding to the plateau and the peak of the spike were determined using the experimental data on the respective radiance temperatures and the melting point of niobium, 2750 K [4]. Different surface roughnesses were achieved by using different grades of sand paper. The RMS surface roughness was measured with the stylus of the measuring equipment traversing normal to the general direction of the grooves.

A summary of the experimental results is given in Table 1. Emittance differences (corresponding to the radiance temperature difference between the peak of the spike and the plateau) as a function of specimen surface roughness are shown in Figure 2. It may be seen that the difference between the emittances of solid and liquid surfaces at the melting point increases with increasing surface roughness. The linear function in Figure 2 (obtained by the least squares method and forced passage through the origin) is a reasonably good representation of the general trend of the data. The average absolute difference between the data points and the function is 0.9 (in percentage emittance difference), which is within the experimental uncertainties. The slope of the linear function is  $0.177 \mu\text{m}^{-1}$ .

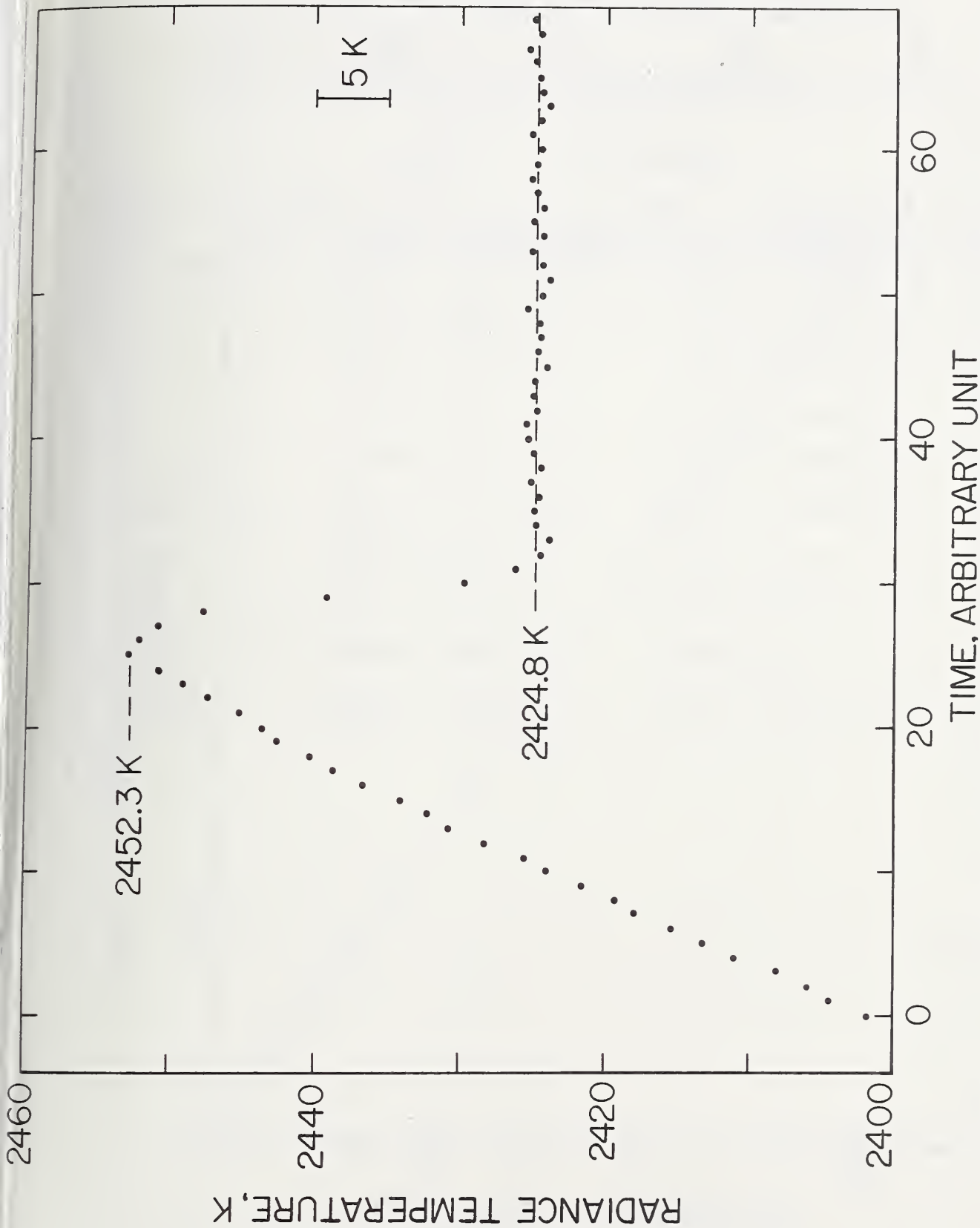


FIGURE 1. Variation of radiance temperature (at 650 nm) as a function of time for a niobium specimen near and at its melting point. Surface roughness is 0.53  $\mu\text{m}$ . One time unit is 0.833 ms.

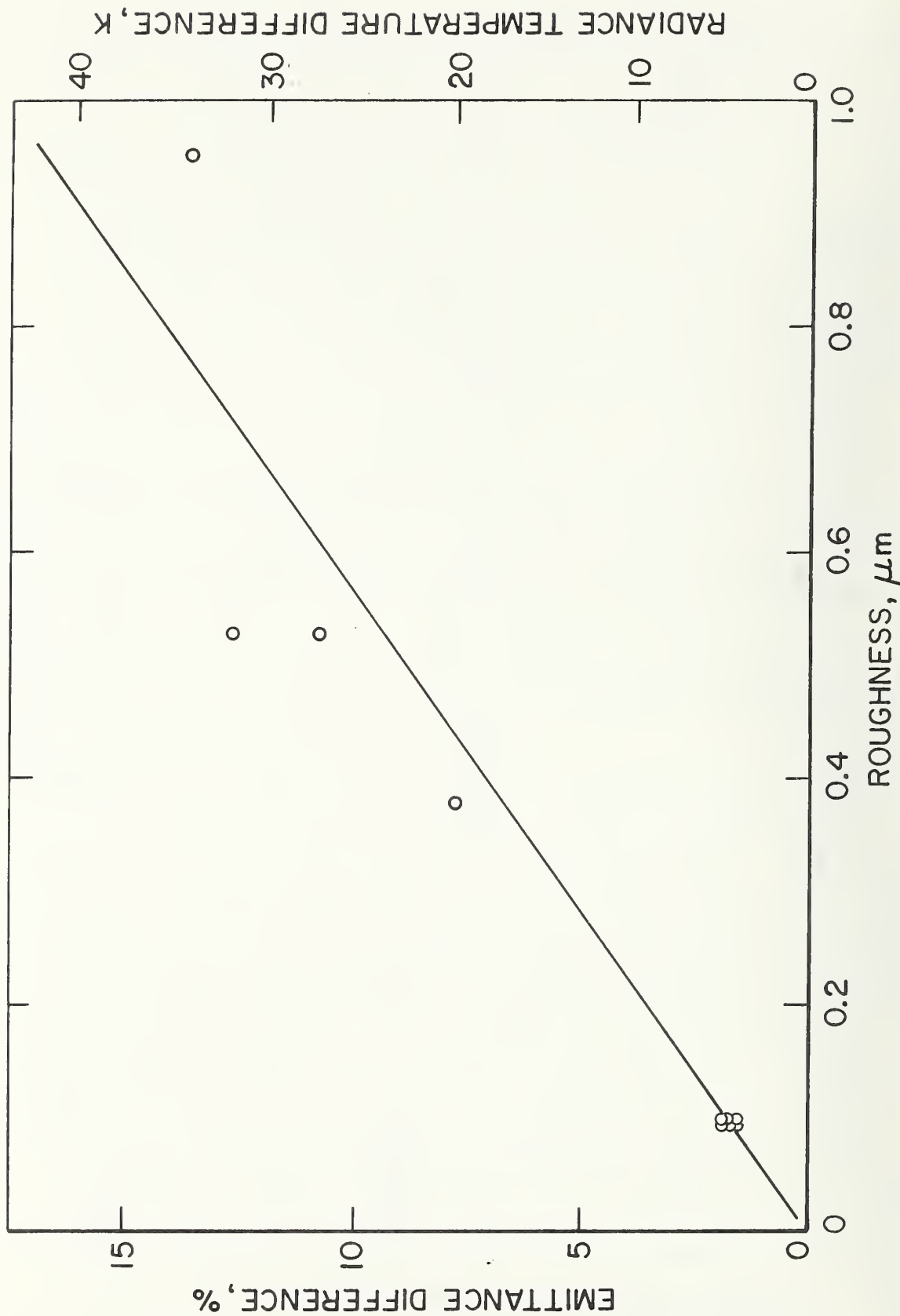


FIGURE 2. Difference in normal spectral emittances (at 650 nm) of solid and liquid niobium at the melting point as a function of solid surface roughness.

Table 1

Summary of Experimental Results for  
Radiance Temperature and Normal Spectral  
Emittance (at 650 nm) of  
Niobium at its Melting Point

Specimen	Roughness $\mu\text{m}$	Radiance Temperature, K			Emittance		
		Peak	Plateau	Diff. (K)	Peak	Plateau	Diff. (%)
1	.38	2444.0	2424.0	20.0	.3650	.3387	7.76
2	.10	2429.7	2424.9	4.8	.3461	.3399	1.82
3	.10	2430.1	2425.6	4.5	.3466	.3408	1.70
4	.53	2456.5	2424.5	32.0	.3822	.3394	12.61
5	.95	2460.3	2425.2	35.1	.3876	.3403	13.90
6	.53	2452.3	2424.8	27.5	.3764	.3398	10.77
7	.10	2429.9	2425.9	4.0	.3463	.3412	1.49
8	.10	2428.9	2424.2	4.7	.3450	.3390	1.77
9	.10	2429.6	2425.2	4.4	.3459	.3403	1.65
10	.10	2429.7	2425.8	3.9	.3461	.3410	1.50

The fact that emittance difference approaches zero as the roughness parameter approaches zero indicates that the primary reason for the change in emittance during melting is the change in surface conditions and not the change in the intrinsic properties of the specimen. At this time, this may be said to apply to niobium based on the results of a limited number of experiments. Additional work on other elements is necessary in order to generalize the above conclusion.

#### References

- [1] Cezairliyan, A., Morse, M. S., Berman, H. A., and Beckett, C. W., J. Res. Nat. Bur. Stand. (U. S.), 74A (Phys. and Chem.), 65 (1970).
- [2] Cezairliyan, A., J. Res. Nat. Bur. Stand. (U. S.), 75C (Eng. and Instr.), 7 (1971).
- [3] Cezairliyan, A., J. Res. Nat. Bur. Stand. (U. S.), 77A (Phys. and Chem.), 333 (1973).
- [4] Cezairliyan, A., High Temperatures - High Pressures, 4, 453 (1972).

## Chapter 6

### RADIANCE TEMPERATURE OF NIOBIUM AT ITS MELTING POINT\*

Ared Cezairliyan

Institute for Materials Research

National Bureau of Standards

Washington, D. C. 20234

#### Abstract

A subsecond duration pulse heating method is used to investigate variations in the radiance temperature (at 650 nm) of niobium near and at its melting point. Measurements were made on several specimens with different surface conditions. The results do not indicate any dependence of radiance temperature (at the melting point) on initial surface conditions. The average radiance temperature (at 650 nm) at the melting point for twelve different niobium specimens is 2425 K on the International Practical Temperature Scale of 1968, with an average absolute deviation of 0.6 K and a maximum deviation of 1.2 K.

---

\*This work was supported in part by the Directorate of Aeromechanics and Energetics of the U. S. Air Force Office of Scientific Research.

## 1. Introduction

In an earlier publication [1]<sup>1</sup>, the application of a millisecond resolution pulse heating technique to the measurement of the melting point of niobium was described. In the same publication, preliminary results for the normal spectral emittance (at 650 nm) of two niobium specimens at the melting point were also presented. Normal spectral emittance was obtained from the measurements of the melting point and the radiance temperature at the melting point.

In general, specimen radiance temperature at a given true temperature is not a reproducible quantity. Radiance temperature depends on specimen surface conditions, thus it varies from specimen to specimen (of the same substance) and it may even be different for the same specimen at different times and under different environments.

However, the preliminary results of radiance temperature measurements for the two different specimens reported in the earlier study [1] were within 1.5 K of each other at the melting point of niobium (2750 K). This has suggested the possibility that radiance temperature (at the melting point) may be independent of surface conditions of the solid specimen, thus it may be a reproducible quantity for pure specimens of similar thermal history.

---

<sup>1</sup> Figures in brackets indicate the literature references at the end of this paper.

The objective of this paper is to further investigate the melting behavior of niobium and to report the results of recent accurate measurements, utilizing a pulse heating technique, of the radiance temperature of niobium near and at its melting point.

## 2. General Considerations

Melting of a pure metal is manifested by a plateau in the temperature versus time curve as shown in figure 1 (Case 1). Since in the figure heating curve is represented by the specimen radiance temperature, validity of the shape of the curve is based on the assumption that normal spectral emittance of the metal does not change during the solid-to-liquid transition. For real surfaces this assumption is not satisfied, and it is likely that one obtains a heating curve similar to the one shown in figure 1 (Case 2). The drop at the beginning of the plateau corresponds to the change in normal spectral emittance of the metal surface as it melts. An initial high radiance temperature (peak of spike) indicates that normal spectral emittance of the solid surface is higher than that of the liquid surface. This is likely to be the case, in general, since solid surfaces, regardless of the degree of polish, depart from the conditions of ideal smoothness.

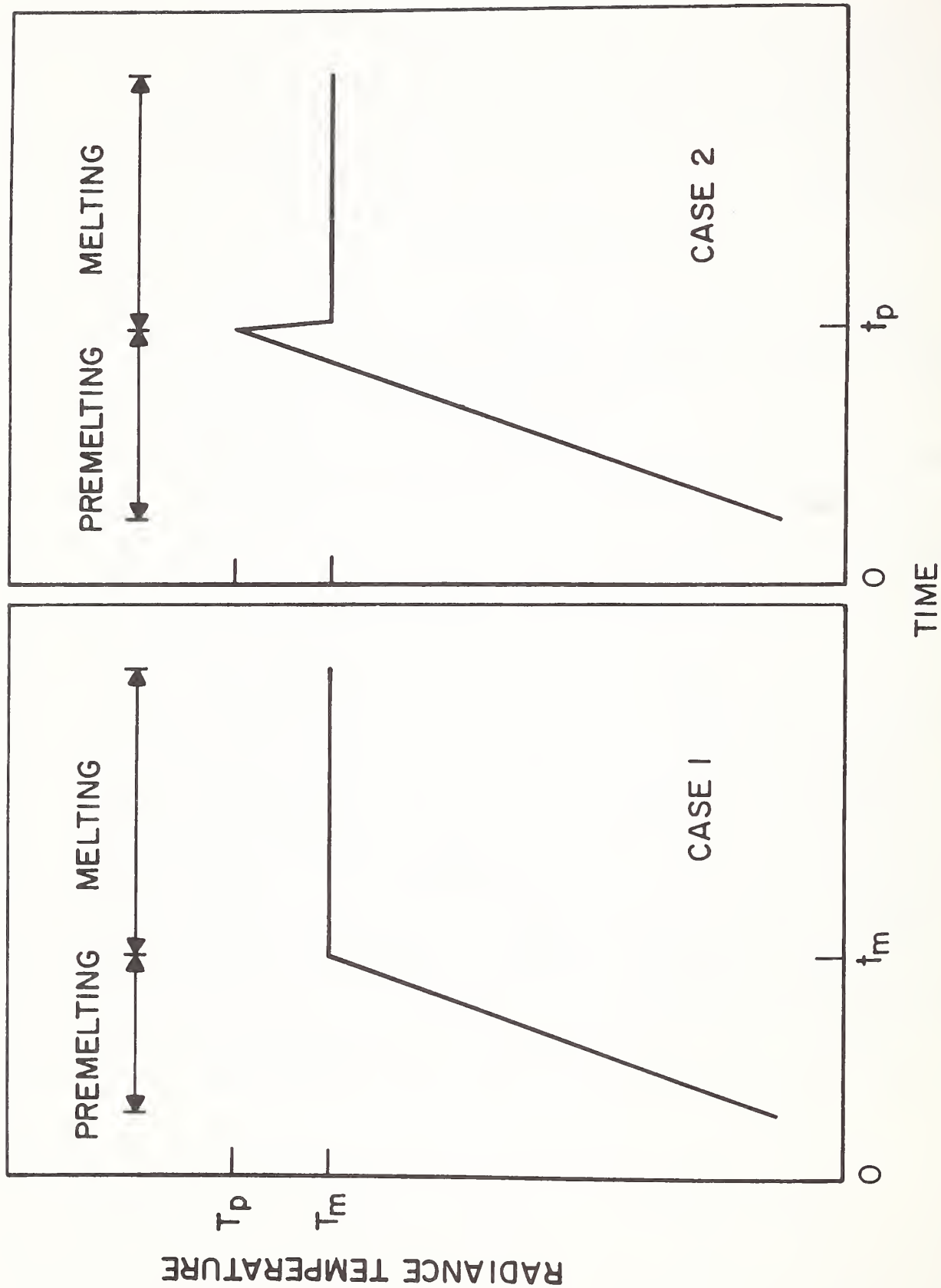


FIGURE 1. Radiance temperature of pure metals near and at their melting points.

### 3. Method

The method is based on resistive self-heating of the specimen from room temperature to its melting point in less than one second and measuring, with millisecond resolution, the pertinent experimental quantities. Specimen's radiance temperature was measured with a high-speed photoelectric pyrometer [2], which permits 1200 evaluations of specimen temperature per second. The radiance measurements were performed at 650 nm which corresponds to the effective wavelength of the pyrometer's interference filter. The bandwidth of the filter was 10 nm. The circular area viewed by the pyrometer was 0.2 mm in diameter. The recordings of temperature were made with a high-speed digital data acquisition system [3], which is capable of recording data at the rate of 2400 per second with a full-scale signal resolution of approximately one part in 8000. Details regarding the construction and operational characteristics of the entire measurement system are given in an earlier publication [4].

### 4. Measurements

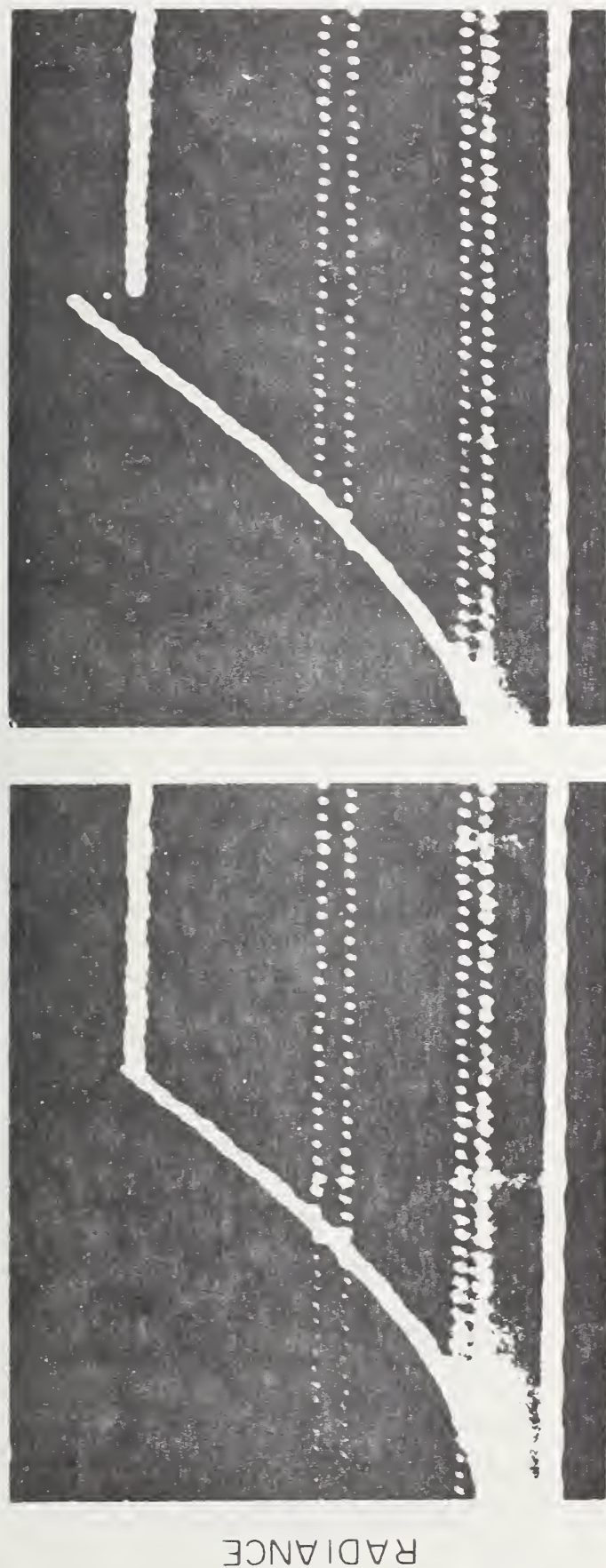
The niobium specimens were in the form of strips with the following nominal dimensions: length, 75 mm; width, 6.3 mm; and thickness, 0.25 mm. All of the specimens were from the same lot and were 99.9<sup>+</sup> percent pure. Manufacturer's analysis indicated the presence of the following impurities in ppm by weight: Ta, 210; Hf and W, <100 each; Fe, Mo and Zr, <50 each; Al, Ca, Cr, Co, Cu, Mg, Mn, Ni, Pb, Si, Sn, Ti, V, <20 each; Cd, <5; O, 42; N, 25; C, 14; H, 5.

A total of twelve experiments were performed on twelve different specimens. Eight of the experiments were conducted on specimens with surfaces ~~in the~~ "as received" conditions (smooth and shiny). The remaining four experiments were performed on specimens with three different surface roughnesses, which were achieved by using different grades of sand paper. The surface roughness of a typical "as received" specimen was  $0.10\text{ }\mu\text{m}$ , and for the others it ranged from  $0.38$  to  $0.95\text{ }\mu\text{m}$ , yielding a factor of approximately ten for the overall variation in surface roughness.

In nine of the experiments the specimens were in a vacuum environment of approximately  $10^{-5}$  torr, and in three of the experiments the specimens were in an argon environment at approximately atmospheric pressure.

The specimens were initially annealed by the manufacturer. Ten of the experiments were performed without any additional heat treatment. In two of the cases, the specimens were further annealed in the laboratory before the experiments by subjecting them to 30 heating pulses (up to  $2400\text{ K}$ ).

Different heating rates, ranging from  $1000\text{ K s}^{-1}$  to  $20,000\text{ K s}^{-1}$ , were used in the experiments. This corresponds to specimen heating periods (from room temperature to the melting point) in the range from  $40\text{ ms}$  to  $800\text{ ms}$ . The magnitude of current pulses near the melting point was in the range from  $200$  to  $600\text{ A}$ . The high-speed pyrometer was calibrated during the period between experiments 7 and 8 against a tungsten filament standard lamp, which in turn was calibrated against the NBS Temperature Standard.



RADIANCE

TIME, 1-50ms-1

FIGURE 2. Oscilloscope trace photograph of specimen radiance near and at its melting point as measured with the high-speed pyrometer. Photograph on the left is for specimen-2 having a "smooth" surface. Photograph on the right is for specimen-5 having a "rough" surface. Radiance is in arbitrary units.

A summary of the experimental procedure is given in table 1. All measurements reported in this paper are based on the International Practical Temperature Scale of 1968 [5].

## 5. Experimental Results

The radiance temperature of niobium at its melting point for the twelve experiments (corresponding to twelve specimens) and other pertinent results are given in table 1. Oscilloscope trace photographs of specimen radiance as measured with the high-speed pyrometer for two typical experiments representing two specimens having different initial surface conditions ("smooth" and "rough") are shown in figure 2. Comparison of the traces in figures 1 and 2 verifies the assumptions made regarding the shape of the traces in figure 1. Figure 3 shows the variation of radiance temperature as a function of time near and at the melting point for five typical experiments. These experiments were selected to represent different specimen surface and operational conditions. All the curves, with the exception of "A", show spikes of varying magnitude. The specimen heating rate in experiments corresponding to curves "B", "C", "D", and "E" were four times slower than that of "A". Thus, the lack of a spike in curve "A" may be attributed to the inability of the system's detecting it. It is interesting to observe that, regardless of the initial surface and operational conditions, radiance temperature at the melting plateau is approximately the same for all the specimens.

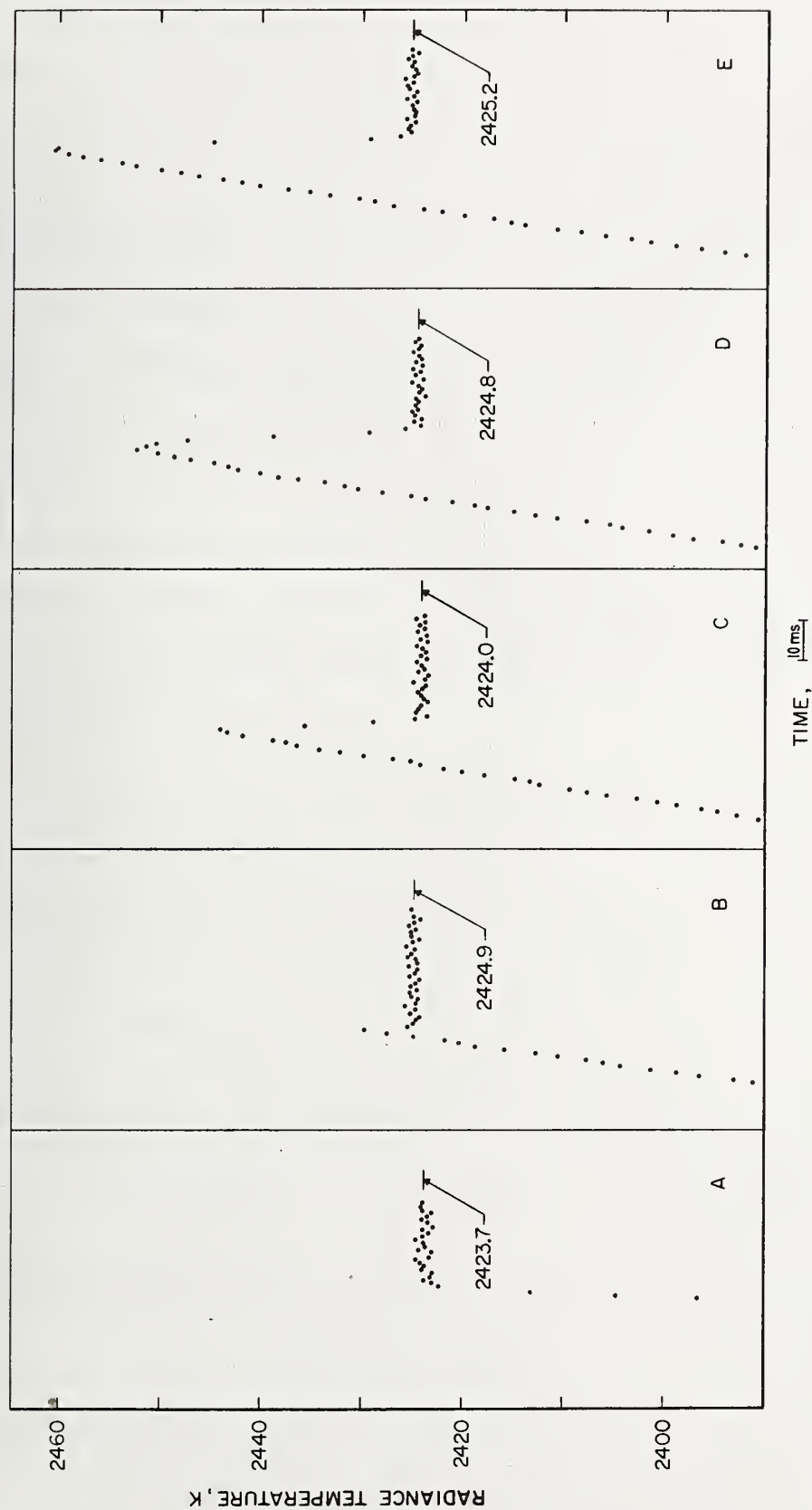


FIGURE 3. Variation of radiance temperature (at 650 nm) of niobium as a function of time near and at its melting point for five typical experiments. Time interval between consecutive temperature points in 0.833 ms.

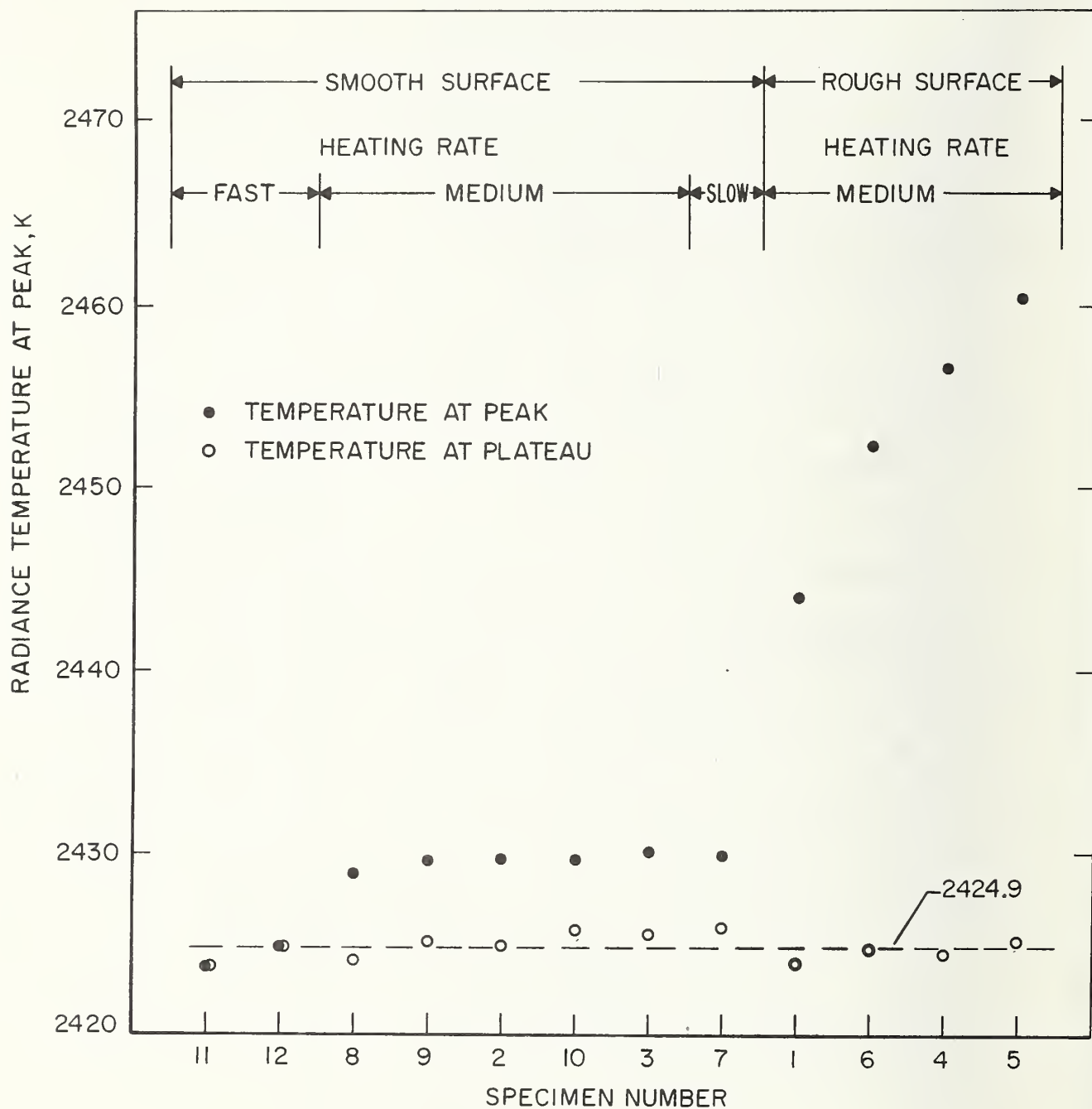


FIGURE 4. Radiance temperature (at 650 nm) at the peak and at the plateau for the niobium specimens.

The results of radiance temperature at the peak of the spike as well as at the plateau for the twelve specimens are shown in figure 4. It may be seen that the two fast experiments do not show any peak for reasons discussed above. For the same "smooth" surface conditions, the results of six experiments give approximately the same value (within 1 K) for the peak temperature, which is 4.4 K higher than the plateau temperature. Further changes in the heating rate (slowing down) did not affect the results. The experiments on specimens with initially rough surfaces yielded high peak temperatures, however, the plateau temperatures were in good agreement (within 1 K) with those of other specimens. The greatest difference between peak and plateau temperatures, corresponding to the specimen with the roughest surface, is 35 K.

A single value for the radiance temperature at the plateau for each specimen was obtained by averaging the temperatures at the plateau. The number of temperatures used for averaging ranged from 12 to 106 depending on the speed of the experiment and the behavior of the specimen during melting. The standard deviation of an individual temperature from the average was in the range from 0.3 to 0.6 K, with the exception of the very fast experiment which yielded 1.4 K. The details of the results for each experiment are given in table 1. To determine the trend of measured temperatures at the plateau, temperatures for each experiment were fitted to a linear function in time using the least squares method. The slopes of the linear functions (table 1) do not show any significant bias with respect to direction. The maximum temperature difference between the beginning and the end of the plateau (corresponding to the slope in the plateau) was in the range from 0.1 to 0.7 K. The standard deviation

Table 1

Summary of experiments for the measurement of radiance temperature of niobium during melting

Specimen Number <sup>a</sup>	Surface Condition <sup>b</sup>	Environment	Premelting Period			Melting Period					Temp. Diff. Peak and Plateau <sup>j</sup> K
			Heating Rate K s <sup>-1</sup>	Stand. Dev. <sup>c</sup> K	Rad. Temp. at Peak <sup>d</sup> K	Number of Temp. <sup>e</sup>	Slope at Plateau <sup>f</sup> K s <sup>-1</sup>	Plateau Temp. Diff. <sup>g</sup> K	Rad. Temp. <sup>h</sup> K	Stand. Dev. <sup>i</sup> K	
1	rough-L	vacuum	2500	0.6	2444.0	37	-14.7	-0.4	2424.0	0.5	20.0
2	smooth	vacuum	2900	0.5	2429.7	90	2.4	0.2	2424.9	0.4	4.8
3	smooth	vacuum	2800	0.5	2430.1	92	-3.6	-0.3	2425.6	0.5	4.5
4	rough-M	vacuum	2800	0.4	2456.5	31	-9.3	-0.2	2424.5	0.5	32.0
5	rough-H	vacuum	2700	0.4	2460.3	30	-11.6	-0.3	2425.2	0.3	35.1
6	rough-M	vacuum	2600	0.5	2452.3	91	9.9	0.7	2424.8	0.6	27.5
7	smooth	vacuum	1000	0.5	2429.9	106	-0.8	-0.1	2425.9	0.4	4.0
8	smooth	vacuum	3000	0.4	2428.9	54	6.3	0.3	2424.2	0.3	4.7
9	smooth	vacuum	2300	0.4	2429.6	95	-7.0	-0.6	2425.2	0.4	4.4
10	smooth	argon	2400	0.5	2429.7	32	-13.3	-0.4	2425.8	0.5	3.9
11	smooth	argon	11400	0.6	2423.7	20	-7.6	-0.1	2423.7	0.5	0
12	smooth	argon	20700	0.6	2424.9	12	10.3	0.1	2424.9	1.4	0

<sup>a</sup>Also represents the experiments in chronological order.

<sup>b</sup>The notations used for surface conditions correspond to the following typical roughnesses in  $\mu\text{m}$ : smooth, 0.10; rough-L, 0.38; rough-M, 0.53; rough-H, 0.95.

<sup>c</sup>Represents standard deviation of an individual temperature as computed from the difference between the measured value and that from the smooth temperature versus time function (quadratic) obtained by the least squares method. Data extends approximately 100 K below the melting point.

<sup>d</sup>Maximum radiance temperature that corresponds to the peak of the spike in temperature observed just before melting of specimen.

<sup>e</sup>Number of temperatures used in averaging the results at the plateau to obtain an average value for the radiance temperature at the melting point of the specimen.

<sup>f</sup>Derivative of the temperature versus time function obtained by fitting the temperature data at the plateau to a linear function in time using the least squares method.

<sup>g</sup>Maximum radiance temperature difference between the beginning and the end of the plateau based on the linear temperature versus time function.

<sup>h</sup>The average (for a specimen) of measured radiance temperatures at the plateau.

<sup>i</sup>Standard deviation of an individual temperature as computed from the difference between the measured value and that from the average plateau radiance temperatures.

<sup>j</sup>Difference between peak and average plateau radiance temperatures.

obtained by this procedure was the same as that obtained by direct averaging of the temperatures.

The results of the radiance temperature at the plateau are shown in figure 5 for two specimens having "smooth" surfaces representing two different heating rates (table 1). The plateaus do not show any anomalies and are horizontal from the beginning to the end. However, the results are somewhat different in the case of specimens having initially rough surfaces (figures 6). Temperature instabilities are observed during the initial melting period, which subside during the second half yielding a horizontal plateau. The temperatures in the anomalous region are approximately 1 to 3 K above those at the stable plateau.

The average radiance temperature at the melting point for the twelve specimens was 2424.9 K, with an average absolute difference of 0.6 K and a maximum difference of 1.2 K. The results are presented in figure 7. It may be concluded that the radiance temperature (at 650 nm) of niobium at its melting point is 2425 K.

## 6. Estimate of Errors

The details of sources and estimates of errors in high-speed experiments similar to those conducted in this study are given in an earlier publication [3]. Specific items in the error analysis were recomputed whenever the present conditions differed from those

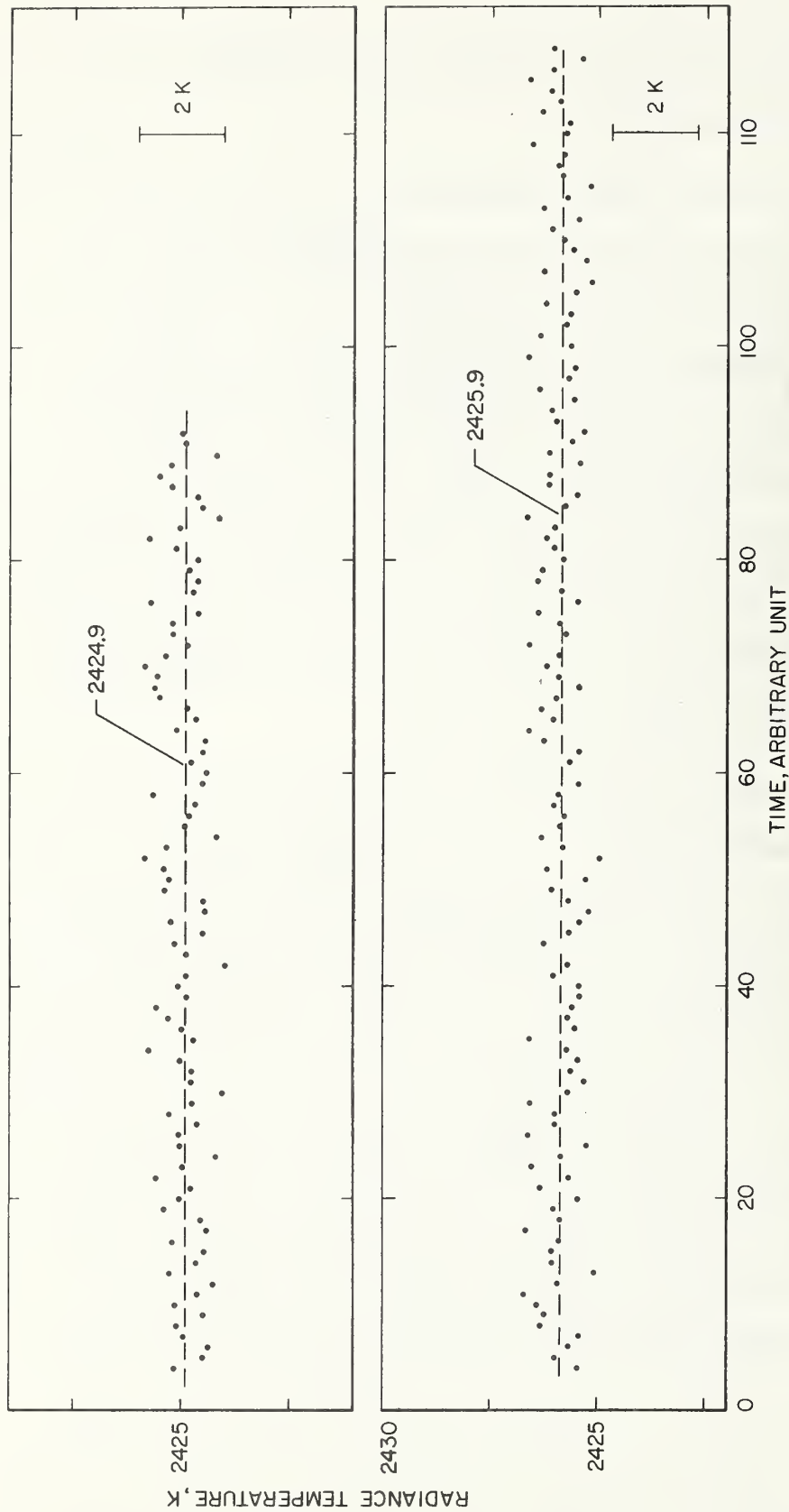


FIGURE 5. Radiance temperature (at 650 nm) of niobium (with initially "smooth" surface) at its melting point. Upper trace is for specimen-2, and lower trace is for specimen-7. One time unit is 0.833 ms.

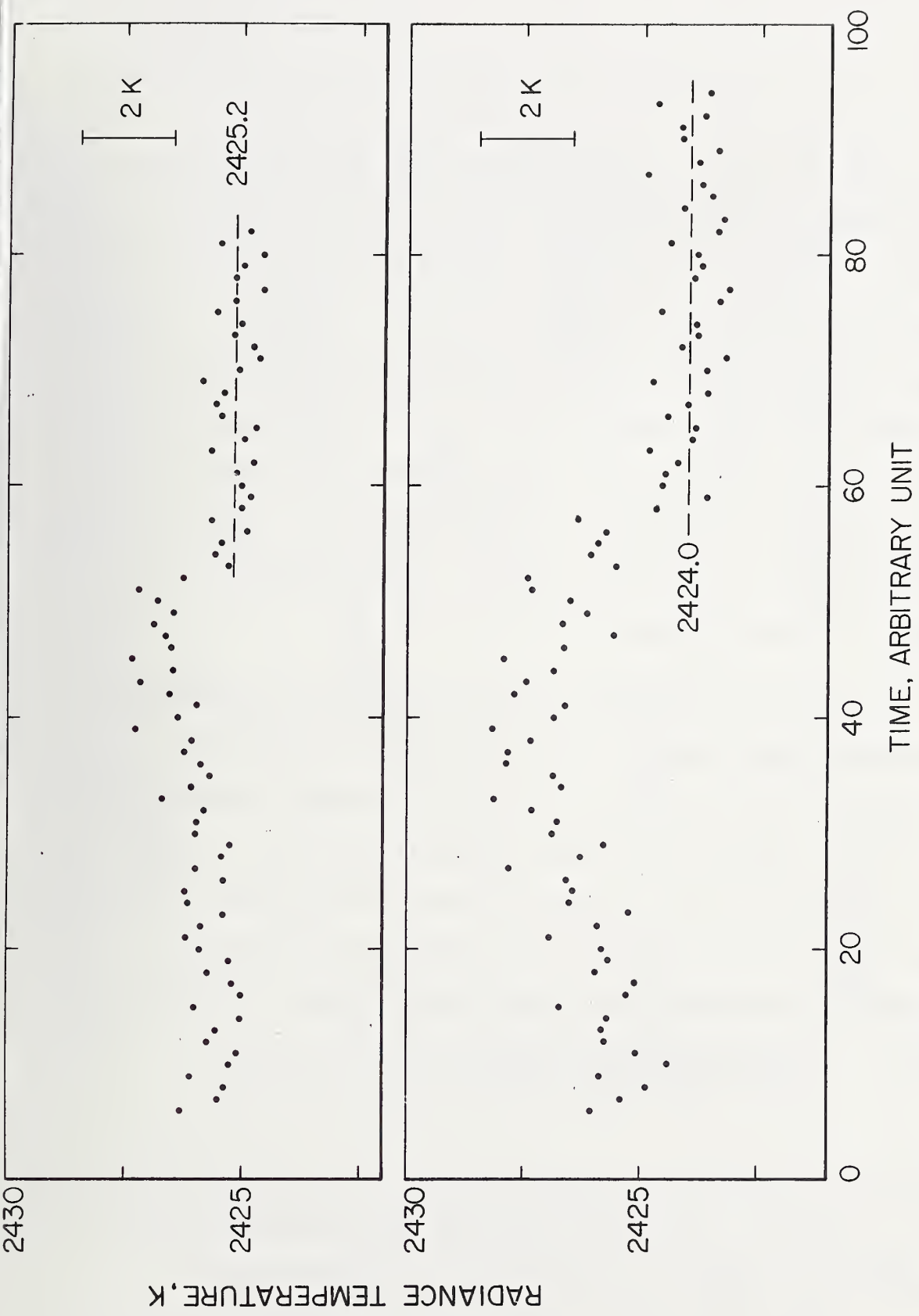


FIGURE 6. Radiance temperature (at 650 nm) of niobium (with initially "rough" surface) at its melting point.

in the earlier study. The imprecision<sup>2</sup> of temperature measurements, during heating as well as melting periods, is approximately 0.5 K (table 1). Inaccuracy<sup>3</sup> of temperature measurements near and at the melting point of niobium is estimated to be not more than 7 K. The major single source contributing to this inaccuracy is the uncertainty in the calibration of the tungsten filament standard lamp (approximately 3 K at 2400 K). The melting point depression due to the impurities in the specimens is estimated to be not more than 2 K. It may be concluded that the inaccuracy of measured radiance temperature of niobium at its melting point is not more than 10 K.

It may be seen from table 1 that the imprecision of temperature measurements during heating of the specimen (before reaching the melting point) was approximately the same as that during the melting period. This indicates that in the experiment the initial melting phase progressed normally and that there were no undesirable effects during melting of the specimen, such as vibration of the specimen, instantaneous development of hot spots in the specimen, and random changes in the specimen surface conditions.

---

<sup>2</sup>Imprecision refers to the standard deviation of an individual temperature as computed from the difference between the measured value and that from the smooth function obtained by the least squares method.

<sup>3</sup>Inaccuracy refers to the estimated total error (random and systematic).

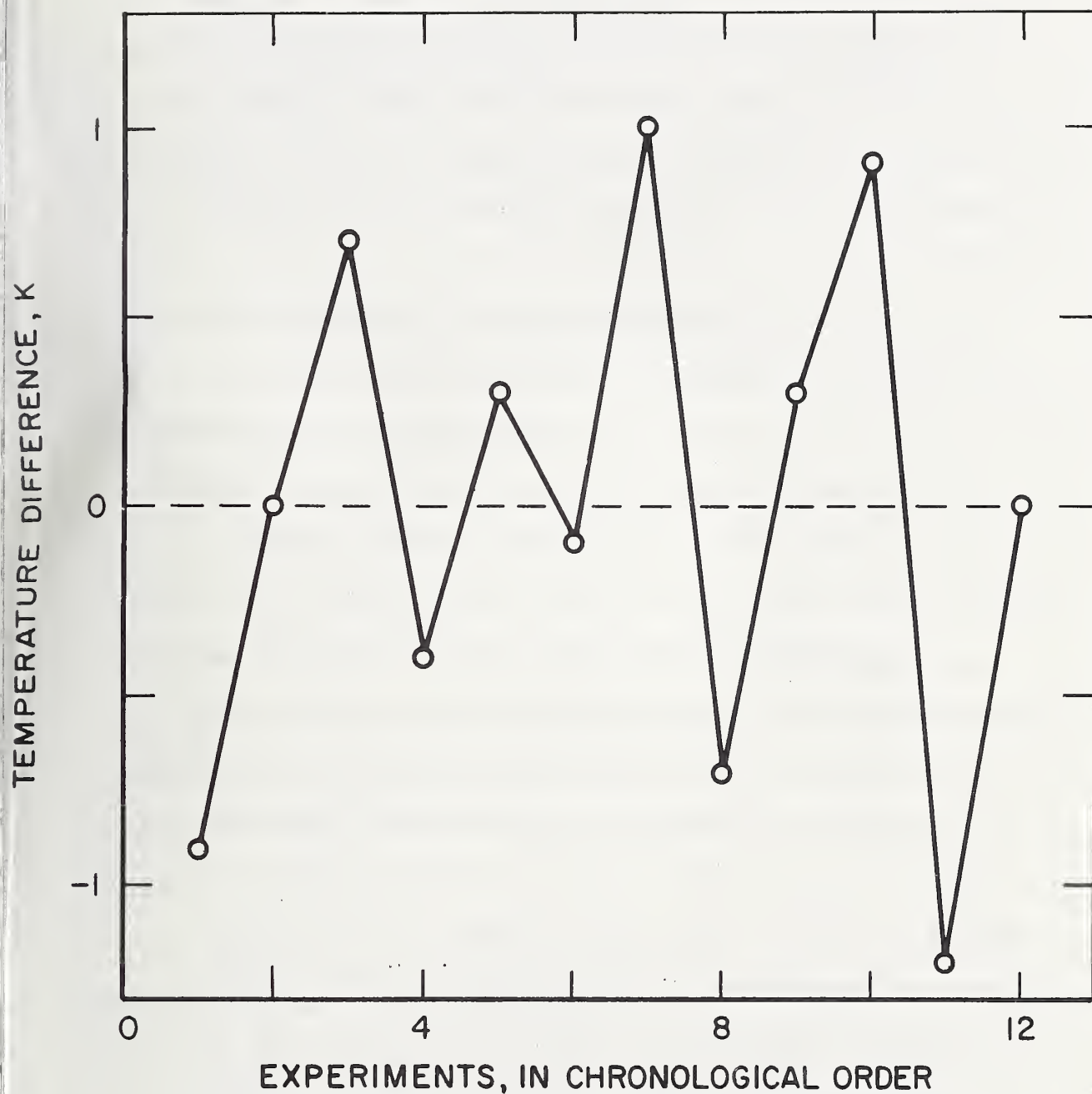


FIGURE 7. Difference of radiance temperature (at the melting point of niobium, at 650 nm) for individual experiments from their average value of 2424.9 K (represented by the "zero" line).

## 7. Discussion

The results of this study show that radiance temperature at the melting point of niobium is reproducible and is independent of: (a) the initial surface conditions of the specimen, (b) the environment in which the specimen is heated, and (c) the heating rate of the specimen.

The twelve experiments performed under different conditions yielded an average value of 2424.9 K for the radiance temperature, with an average absolute difference of 0.6 K and a maximum difference of 1.2 K. The preliminary results on two niobium specimens reported in an earlier publication [1] had yielded an average value of 2423.3 K, which is only 1.6 K below the present value.

Considering 2750 K for the melting point of niobium [1] and 2425 K for the radiance temperature at the melting point, a value of 0.340 is obtained for the normal spectral emittance (at 650 nm) at the melting point of niobium. Earlier measurement, utilizing the same pulse heating system, on tubular niobium specimens in the range 1700 to 2300 K showed a linear variation of normal spectral emittance with temperature [6]. Extrapolation of these results to the melting point yields 0.348 for normal spectral emittance, which is approximately 2 percent higher than the present value. Measurement of normal spectral emittance of niobium near its melting point is reported in the literature to be 0.362 [7]; this is approximately 6 percent higher than the present value. In the case of solid surfaces departure, in varying degrees, from ideal surface conditions may have been partially responsible for the high values.

This may be demonstrated by considering the present results on "rough" specimens. From table 1 (last column) it may be seen that for the "rough" specimens a considerable difference exists between the peak and plateau temperatures. This difference in temperature corresponds to a difference in normal spectral emittance ranging from 7 to 14 percent for the four "rough" specimens. In the case of the "smooth" specimens, corresponding average difference in emittance is approximately 2 percent. The above substantiate, both in magnitude and in direction, the difference between present results and those reported in the literature.

Radiance temperature (at 645 nm) <sup>of</sup> liquid niobium at its melting point was measured recently using a lavitation calorimeter [8]. The reported result of 2405 K is 20 K lower than the present value. No satisfactory explanation has been found for this discrepancy.

It may be noted that, with the present system it was not possible to follow the entire melting process because the specimen collapsed and opened the main electrical circuit prior to the completion of melting.

In conclusion, the results of this study have shown the constancy and reproducibility of the radiance temperature of niobium at its melting point. Compared to the difficulties encountered in the construction and operation of blackbody cavities at temperatures above 2000 K, the scheme of measuring radiance temperature at the melting point of selected substances may be an easier, more accurate, and in addition more practical approach for performing secondary calibration on instruments and for conducting overall

on-the-spot checks on complicated measurement systems at high temperatures. This suggests the extension of investigations, similar to those reported in this paper, to other refractory metals at temperatures above 2500 K.

## 8. References

- [1] Cezairliyan, A., Measurement of melting point, normal spectral emittance (at melting point), and electrical resistivity (above 2650 K) of niobium by a pulse heating method, High Temperatures-High Pressures, in press.
- [2] Foley, G. M., High-speed optical pyrometer, Rev. Sci. Instr., 41, 827 (1970).
- [3] Cezairliyan, A., M. S. Morse, H. A. Berman, and C. W. Beckett, High-speed (subsecond) measurement of heat capacity, electrical resistivity, and thermal radiation properties of molybdenum in the range 1900 to 2800 K, J. Res. Nat. Bur. Stand. (U.S.), 74A (Phys. and Chem.), 65 (1970).
- [4] Cezairliyan, A., Design and operational characteristics of a high-speed (millisecond) system for the measurement of thermophysical properties at high temperatures. J. Res. Nat. Bur. Stand. (U.S.), 75C (Eng. and Instr.), 7 (1971).
- [5] International Practical Temperature Scale of 1968, Metrologia, 5, 35 (1969).
- [6] Cezairliyan, A., High-speed (subsecond) measurement of heat capacity, electrical resistivity, and thermal radiation properties of niobium in the range 1500 to 2700 K, J. Res. Nat. Bur. Stand. (U.S.), 75A (Phys. and Chem.), 565 (1971).
- [7] Pemsler, J. P., Thermodynamics of interaction of niobium and tantalum with oxygen and nitrogen at temperatures near the melting point, J. Electrochem. Soc., 108, 744 (1961).

- [8] Bonnell, D. W., J. A. Treverton, A. J. Valerga, and J. L. Margrave, The emissivities of liquid metals at their fusion temperatures, Proceedings of the Fifth Symposium on Temperature, in press.



